

**Examination of intramolecular interactions between residues of the cys-loop GABA
receptor Hco-UNC-49 from *Haemonchus contortus***

By

Josh G. Foster

A Thesis Submitted in Partial Fulfillment

Of the Requirements for the Degree of

Masters of Science

In

The Faculty of Science

Applied Bioscience

University of Ontario Institute of Technology

©Josh G. Foster, 2016

Certificate of approval

Abstract

Haemonchus contortus is a parasitic nematode known to infect ruminant animals such as sheep, goats and cattle. Despite several different anthelmintic drugs available to control the spread of this infection, *H. contortus* has shown resistance to all of them. In order to combat the infection, a novel drug target must be found and characterized. Hco-UNC-49 is unique parasitic nematode γ -aminobutyric acid (GABA) gated chloride channel that may prove to be a novel drug target. The objective of this thesis was to characterize intramolecular interactions of Hco-UNC-49B. Two sets of oppositely charged residues were chosen based on their proximity to each other in a model of Hco-UNC-49 generated using the *C. elegans* GluCl crystal structure as a template. These residues are predicted to form salt bridges in Hco-UNC-49B which may contribute to structure, function, and molecular interactions with ligands. Each amino acid was mutated to an alanine, followed by a mutation to a similar charged amino acid, and finally a swap between the two residues encompassing the salt bridge. It was found that all residues chosen were critical for receptor function to varying degrees. R159 may be interacting with D83 by either a hydrogen or ionic interaction. Overall, this thesis revealed a probable salt bridge that may be conserved among GABA receptors, as well as one novel interaction that may be unique to Hco-UNC-49. These results expose similarities and differences between Hco-UNC-49 and mammalian GABA receptors that may be vital for the creation of new anthelmintics.

Key words: *Haemonchus contortus*, Ligand-gated chloride channel, Salt bridge, Hco-UNC-49B, GABA, electrophysiology

Acknowledgements

Firstly, I would like to express my sincere appreciation to my advisor Prof. Sean Forrester for the continuous support of my M.Sc., for his patience, motivation, and immense knowledge. I would also like to thank Prof. Forrester for all the times he has been understanding, helping with all the small details, and reassuring me throughout my time with electrophysiology. Besides my advisor, I would like to thank the rest of my thesis committee: Prof. Bonetta, and Prof. Desaulniers, for their insightful comments, knowledge, and encouragement throughout thesis. I also thank my fellow lab mates Ariel Kwaka, Everett Cochrane, and Micah Callanan for the stimulating discussions, inside jokes, and for all the enjoyment we have had during my time in the Forrester lab. I would also like to thank the undergraduate students that have helped to bring this project along, in particular, David Au.

I would like to thank my friends and family for putting up with me throughout this research study, for helping me, guiding me, and providing me a place to escape. I thank them for all the help they have given me with preparation for this thesis; for practicing presentations, proof reading, and engaging in scientific discussions. Lastly, I would like to thank Kelsey, my girlfriend, for all the support, discussions, proof reading, practising of presentations, feedback, and constant faith in me over the past two years.

Table of contents

1. Introduction and Significance.....	1-2
2. Objectives of the Thesis.....	3
3. Literature Review.....	3-7
3.1. <i>Haemonchus contortus</i> background.....	3
3.2. Distribution of <i>H. contortus</i> and economic concerns.....	4
3.3. Life stages.....	4-6
3.4. Control of <i>H. contortus</i>	6-7
4. Anthelmintic Drugs.....	7-9
4.1. Benzimidazoles.....	7-8
4.2. Imidazthiazoles.....	8
4.3. Macrocyclic lactones.....	8
4.4. Other classes of Anthelmintic drugs.....	8-9
5. Ligand-Gated Ion Channels.....	10-18
5.1. GABA receptors.....	12-14
5.2. GABA receptors in nematodes.....	14-15
5.3. GABA receptors in <i>H. contortus</i>	15-18
6. Methods.....	19-24
6.1. UNC-49B mutant primer design.....	19-20
6.2. cRNA production of UNC-49B mutants.....	21-22
6.3. Expression of UNC-49B mutants in <i>X. laevis</i> oocyte.....	22
6.4. Two-electrode voltage clamp electrophysiology.....	22-23
6.5. Modelling.....	23-24
6.6. Substituted Cysteine Accessibility Method.....	24
7. Results.....	25-34
7.1. Electrophysiology of mutants.....	26-27
7.2. D83 mutations.....	27-28
7.3. H137 mutations.....	28-29
7.4. R159 mutations.....	29-30
7.5. E183 mutations.....	31

7.6. E185 mutations.....	31
7.7. R241 mutations.....	32
7.8. Swap mutations.....	32-33
7.9. Modelling results.....	33-34
8. Discussion.....	35-41
8.1. Salt-bridges.....	36-41
9. Conclusion.....	42-44
9.1. Impact and conclusion.....	43-44
10. References.....	45-53
11. Appendices.....	54-62
11.1. Primers.....	55-57
11.2. Characterization of Loop E residues utilizing the Substituted Cysteine Accessibility Method.....	57-58
11.3. Characterization of Hco-UNC-49 utilizing GABA Analogues.....	59-61
11.4. Pharmacological study of D83T.....	61-62

List of Tables

Table 1. Charged residue mutations of potential salt bridges. EC₅₀ are compared for the heteromeric UNC-49B/C receptor with GABA. pg 27

Table 2. Distances between residues of the predicted salt-bridges of UNC-49B. pg 35

Table 3. Summary of the comparison of residues between Hco-UNC-49B and the Human GABA_A receptors including the specific interactions found in GABA_A. pg 42

Appendices:

Table 1. Hco-UNC49B charged residue mutagenesis primers. Each mutagenesis primer name indicates the residue to be mutated, the position in the sequence, and the new residue in the mutant. Primers were designed using Stratagene's web-based QuikChange® Primer Design Program. pg 55-57

Table 2. GABA analogues to be used on the WT (wild-type) UNC-49 channel of *H. contortus*. pg 59

Table 3. EC₅₀ calculations of the two GABA analogues known as Molecule B (TACA) and Molecule D (4-(hydroxyamino)-4-oxobutan-1-aminium) are compared to the heteromeric UNC-49B/C receptor with GABA. pg 60

List of Figures

Figure 1. Image portraying the life cycle of *Haemonchus contortus*. L1 through L3 are the free living nematode. *L3 represents transition from free-living to parasitic life stages in which the nematode becomes unsheathed. L4 and the adult worm are parasitic. Eggs are laid in the host but are excreted by the host to develop into L1 free- living nematodes. Created by Josh Foster as a summary from Veglia, 1915. pg 6

Figure 2. Examples of different anthelmintic drugs. Created by Josh Foster. pg 9

Figure 3. Representation of the pentameric channel with ion flow direction (top). The individual subunit can be seen represented with the 4 transmembrane domains 1 through 4. The orange line represents the disulfide bond of the cys-loop (bottom). Created by Josh Foster. pg 12

Figure 4. Chemical structure of Gamma-Aminobutyric acid (GABA). Created by Josh Foster. pg 14

Figure 5. Left: Side view of the crystal structure of human GABA_A-B3 channel. Right: Top-down view of the GABA_A-β3 channel. PDB 4COF (Miller et al., 2014). pg 14

Figure 6. Model representative of the *Haemonchus contortus* UNC-49B homomeric channel with the 6 loops represented on the primary (A-C) and complimentary subunits (D-F). Created by Micah Callanan. pg 17

Figure 7. Left: Residues for the proposed salt bridges shown in relation to their positions on both the primary (chain A) and complimentary subunits (Chain B). Right: Close up of the proposed salt bridges with distances and labelling of the residues. Created by Micah Callanan. pg 18

Figure 8. Sequence comparison of Hco-UNC-49B with other LGIC for the determination of charged residues. pg 21

Figure 9. pT7Ts vector with *H. contortus unc49* insertion. Created by Josh Foster. pg 22

Figure 10. Two-electrode voltage clamp electrophysiology set up with GABA and ND96 as the solution in and the waste solution out. Created by Josh Foster. pg 23

Figure 11. Dose response curves of D83 mutations. pg 28

Figure 12. Dose response curves of H137 mutations. pg 29

Figure 13. Dose response curves of R159 mutations. pg 30

Figure 14. Results of experimentation with MTSET on R159C mutant. Blue bar is the current before MTSET. Grey bar is after the addition of MTSET. pg 31

Figure 15. Dose response curves of E183 mutations. pg 32

Figure 16. Dose response curves of R1241 mutations. pg 33

Figure 17. Dose response curves of charge reversal mutations. pg 34

Figure 18. A Close up of the relevant residues for the proposed salt bridges with distances and labelling of the residues. Model created by Micah Callanan. pg 35

Appendices:

Figure 1. A: Representative responses before and after MTSET for R159C and T153C at their respective EC₅₀ values. B: Comparison of the percent change of I_{GABA} for each SCAM mutation. pg 58

Figure 2. Dose response curves for the two GABA analogues, Molecule B (TACA) and Molecule D (4-(hydroxyamino)-4-oxobutan-1-aminium). pg 60

Figure 3. A: Representative responses of D83T with GABA, IMA, R-GABOB and S-GABOB at 10mM. EC₅₀ responses for D83T shown with Gabazine underneath. B: Pharmacological results of D83T comparing the responses of each compound relative to GABA. C: Chemical structures of GABA, S-GABOB, R-GABOB and IMA. pg 62

List of Abbreviations

AAD's	amino-acetonitril derivatives
Cel-UNC-49	<i>Caenorhabditis elegans</i> uncoordinated gene 49
cDNA	copy DNA
cRNA	copy RNA
Cys-loop	Cysteine loop
[D]	concentration of agonist
EC ₅₀	half maximal effective concentration
ECD	extracellular domain
GABA	γ -aminobutyric acid
GABA _A	heteromeric vertebrate GABA-gated chloride channel
GABA _C	homomeric vertebrate GABA-gated chloride channel
GluCl	Glutamate-gated chloride channel
Hco-UNC-49B	<i>H. contortus</i> uncoordinated gene 49 homopentameric receptor
Hco-UNC-49BC	<i>H. contortus</i> uncoordinated gene 49 heteromeric receptor
ICD	intercellular domain
IMA	imidazole 4-acetic acid
I _{GABA}	current elicited from GABA activation of GABA gated channel
LGCC	ligand gated chloride channel
LGIC	ligand gated ion channel
MTSET	2-hydroxyethylthiosulfonate
n	number of replicates
RDL	GABA-gated chloride channel in <i>Drosophila melanogaster</i>
R-GABOB	(R)-(-)-4-Amino-3-hydroxybutyric acid
S-GABOB	(S)-(+)-4-Amino-3-hydroxybutyric acid
SCAM	substituted cysteine accessibility method
S.E.	standard error
TEVC	two-electrode voltage clamp
TMD	transmembrane domain

Introduction

1. Introduction and significance

The infections caused by parasitic nematodes is a significant economic burden to the wool, milk and food industry. *Haemonchus contortus* is a parasitic nematode that infects sheep and other ruminant animals by feeding on their blood while in the host's abomasum (Schwarz et al., 2013). There are many anthelmintic drugs that have been used to combat this infective parasite. However, overuse and reliance on these drugs have resulted in increased resistance (O'Connor et al., 2006). Therefore, in order to counter infections caused by *H. contortus*, new anthelmintics must be found. One target for such treatment is the nematode GABA receptor, which differs from the GABA receptors found in the mammalian host (Schuske et al., 2004). The *H. contortus*' GABA receptor, Hco-UNC-49, is composed of five subunits each with four transmembrane domains including a cys-loop and, when bound together, form a pentameric chloride channel (Connolly et al., 2004). The subunit dimers are composed of loops A to C on the principle subunit, and loops D to F on the complementary subunit. Together, these loops form the agonist binding site. The wildtype channel requires both Hco-UNC49-B and C subunits forming a heterodimeric channel. Using many techniques such as sequence homology, modelling and electrophysiology, the nematode GABA receptor can be characterized and further understood both in sequence and function. Many studies have already determined specific residues important in GABA binding; however, further characterization of the intramolecular interactions, such as salt bridges, is still required.

Salt bridges are composed of two oppositely charged amino acid residues which are close enough (within 4.0Å) to experience electrostatic attraction (Bosshard et al., 2004) and in which one pair of heavy atoms is within hydrogen bonding distance (Donald et al., 2011). These salt bridges can contribute to protein structure, the specificity of interactions with the proteins, and

interactions with other biomolecules (Bosshard et al., 2004). The net electrostatic free energy of a salt bridge can be separated into three components: charge-charge interactions, interactions of charges with permanent dipoles and desolvation of charges (Bosshard et al., 2004).

The aim of this thesis research was to help in further characterization and understanding of Hco-UNC-49 which will aid in the production of novel drug candidates to target *H. contortus*' GABA receptors and provide a treatment option for infected animals.

2. Objectives of the Thesis

The main objective of the thesis was to examine intramolecular interactions between residues of the Hco-UNC-49 receptor using *in silico* modeling and site-directed mutagenesis. The mutations were chosen by determining the distances between two residues using a homology model of Hco-UNC-49. Only charged residues were included for analysis. These mutations included mutations of each residue to an alanine, then a mutation to a residue with a charge similar to the wild type residue, and finally a swap mutation was utilized to attempt to rescue the receptor's function. This approach determines potential intramolecular interactions between residues possibly involved in the unique structure and function of Hco-UNC-49.

3. Literature Review

3.1 Haemonchus contortus background

Haemonchus contortus is a nematode parasite that spends its parasitic life stages in the abomasum of ruminants such as sheep and goats. *H. contortus*, otherwise known as the barber's pole worm, is a strongylid nematode which is transmitted orally from one host's excrement to another (Schwarz et al., 2013). The parasite attaches to the wall of the abomasum and feeds on the blood of the animal. This infection is known as haemonchosis and causes many different

health complications including anemia, hypoproteinemia, edema, and weakness; the infection may even result in death (Manninen et al., 2008).

3.2 Distribution of H. contortus and economic concerns

This infection presents many health concerns for the infected hosts and can contribute to economic and industrial losses worldwide. These include reduction of quantity and quality of wool, decreased milk production, and decreased reproduction resulting in decreased meat and herd sizes (Qamar et al, 2011).

Typically, *H. contortus* is seen in tropical and subtropical areas; however, as of 2008, *H. contortus* was found in the northern regions of Finland. While it has been found in Finland since 1933, it has not been found this far north in Finland until recently. In Sweden, *H. contortus* was detected near the Arctic Circle. Due to the arrested development of the fourth larval stage, the parasite is able to survive the winter while within a host (Manninen et al., 2008). While the infection is generally confined to ruminants, there are cases in which *H. contortus* has infected humans (Roberts, 2000; Pestechian et al., 2014).

Over-use and reliance on anthelmintic drugs across the world has resulted in resistance to many treatments. Consequently, haemonchosis has a severe economic impact. In 2011, Qamar et al. showed that parasitic nematodes cost Australia up to \$369 million annually. As well, *H. contortus* was shown to cost \$26m, \$46m, and \$103m for Kenya, South Africa and India respectively, because of loss of body weight, wool, meat, milk and the susceptibility to other infections.

3.3 Life stages

In 1915, Veglia described in full detail the growth and development of *H. contortus*. The parasitic nematode has five stages in its life cycle. Each stage can be divided into two substages, one of activity, and one of lethargy, in which they undergo structural changes. The first two stages, as well as half of the third stage, are free living. Part of the third stage, through to the fifth stage occur within the host as a parasite. *H. contortus* begins its life cycle as an egg laid in the abomasum of a ruminant animal (Figure 1). These eggs require oxygen and are excreted by the host. The eggs hatch outside of the host in the feces and develop into the first-stage larvae (L1). The L1 larvae continue to develop through two molts to the L2 larvae and eventually the L3 larvae, where they are capable of climbing blades of grass using water droplets. The L3 larvae are ingested by the new host where they become unshathed and develop into an L4 larvae (Roeber et al., 2013). The L4 larvae are able to enter a state of hypobiosis, an arrested stage of development (Veglia, 1915). This is dependent on many factors including seasonal, host-immunity and parasitic factors (Veglia, 1915). The L4 larvae will then develop into the mature adult worms. The adult female is capable of laying 4500 eggs daily and can grow up to 30 mm long, whereas the male adult worm can only grow up to 18 mm long (Coyne and Smith., 1992; Nikolaou and Gasser., 2006).

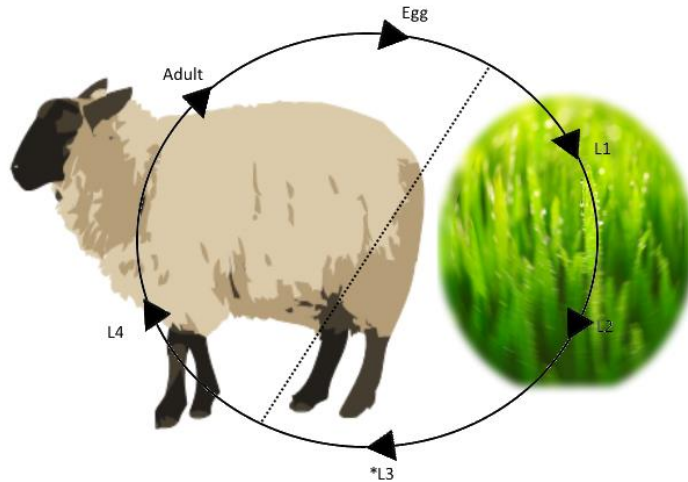


Figure 1. Image portraying the life cycle of *Haemonchus contortus*. L1 through L3 are the free living nematode. *L3 represents transition from free-living to parasitic life stages in which the nematode becomes unsheathed. L4 and the adult worm are parasitic. Eggs are laid in the host but are excreted by the host to develop into L1 free-living nematodes. Created by Josh Foster as a summary from Veglia, 1915.

Temperature and moisture are key factors which influence the development of *H. contortus*. The eggs and initial larval stages are very susceptible to lower temperatures and lack of moisture. *H. contortus* generally survives in areas with summer-dominant temperatures and rainfall. This includes large areas of Asia, India, Africa, Australia, China and America. These areas tend to have warmer temperatures and moisture. However, there has been an increase of incidences of infection in more northern countries such as Sweden, France, Denmark and the Netherlands. This is thought to be due to the hypobiosis of the L4 larvae (O'Connor et al., 2006). It has been noted that the L3 larvae is capable of surviving up to 6 months with optimal temperature and moisture, while the adult worm can only survive several months inside of its host (Veglia, 1915), but long enough to survive cold winters (Qamar et al, 2011).

3.4 Control of *H. contortus*.

One of the most prominent methods of treating haemonchosis is the use of anthelmintic drugs. However, the over-use and unnecessary treatments with these drugs has caused an

increase in resistance in parasitic nematodes (O'Connor et al., 2006). As of 2009, *H. contortus* was known to be resistant to all known anthelmintics with only one exception, amino-acetonitril derivatives (AAD's) (Kaminsky et al., 2008). This resistance and over reliance on anthelmintics has resulted in the need to find alternatives to manage the infections without the use of these chemotherapeutics (O'Connor et al., 2006).

Integrated parasite management (IPM) focuses on using specific environmental conditions to control the spread of infection (O'Connor et al., 2006). IPM generally targets the free living life stages rather than the parasitic stages (O'Connor et al., 2006). This involves intensive rotational grazing and higher stocking rates to reduce close grazing and consumption of parasites. The use of rotational grazing systems is very effective to reduce the amount of time that the ruminant animals spend on specific fields which will decrease the chance of infection and allow for more environmental control over the fields (O'Connor et al., 2006). This way, the immediate environmental conditions can be used to reduce the chance of infection (O'Connor et al., 2006).

4. Anthelmintic Drugs

Anthelmintic drugs are used to treat animals with parasitic worm infections. These worms (including trematodes, cestodes and nematodes) may infect humans, livestock and domesticated pets. Anthelmintic drugs have been over-used, resulting in high resistance in many parasitic worms (Roeber et al., 2013). Despite the fact that IPM methods are becoming more necessary for controlling the spread of *H. contortus*, a treatment option for infected animals is still necessary. There is little motivation for development of new anthelmintics because most nations that require the drugs do not have the money to invest in drug discovery (Holden-Dye et al., 2005). The drug ivermectin has been quite successful over the past 30 years and resulted in a

decreased pressure for alternative anthelmintics until recently (Holden-Dye et al, 2005). There are only a small number of different classes of anthelmintics which are separated by their chemical characteristics (examples in Figure 2), many of which act on ligand gated ion channels. There are three major classes used in veterinary medicines. These are summarized below.

4.1 Benzimidazoles

Benzimidazoles are broad spectrum anthelmintics which act on β -tubulin and prevent the formation of microtubules (Lacey, 1990). Tubulin is required for organelles involved in motility, division and secretion as well as glucose uptake and emptying of glycogen reserves (Lacey, 1990). Benzimidazoles also affects egg production. Examples include thiabendazoles, mebendazole, and fenbendazole .

4.2 Imidazthiazoles

These anthelmintic drugs act as an agonist for the nicotinic acetylcholine receptors (nACh) in nematodes (Holden-dye, et al., 2014). This causes spastic muscle paralysis due to over activation of the receptors (Holden-dye, et al., 2014). They also indirectly target acetylcholinesterase inhibitors (Harder et al., 2003). An example of an imidazthiazole is the drug Levamisole.

4.3 Macrocyclic lactones

Macrocyclic lactones are composed of two different subclasses of anthelmintics which are both thought to act on glutamate-gated chloride channels (GluCl_s), as well as GABA channels (Forrester et al., 2002; Crump et al. 2011). These subclasses include avermectins and milbemycins. Examples include ivermectin, used in livestock, as well as moxidectin which is used in livestock as well as cats and dogs (Harder et al., 2003). Ivermectin is a very potent drug

which causes paralysis of the nematode pharyngeal and body wall musculature (Holden-dye, et al., 2014).

4.4 Other classes of Anthelmintic drugs

There are other smaller classes of anthelmintics. These include examples such as piperazine, which acts on GABA receptors; spiroindoles which cause paralysis by acting as an antagonist for acetylcholine receptors; cyclooctadepsipeptides which are thought to act on calcium and potassium-dependent mechanisms; flavonoids which are found to be associated with DAF-16 activation; spiroindolines which act on the vesicular acetylcholine transporter, UNC-17; aminophenylamidines which act on AChR; Cry proteins from *Bacillus thuringiensis* which are pore forming proteins; nitazoxanide which acts as a pyruvate ferredoxin oxio reductase inhibitor; and fluoroalkenyls which have a broad range of effects. There are also amino-acetonitril derivatives (ADD's) which act as broad spectrum anthelmintics (Holden-dye et al., 2014). It is thought that ADD's act on nematode specific acetylcholine receptor subunits (Kaminsky et al., 2008).

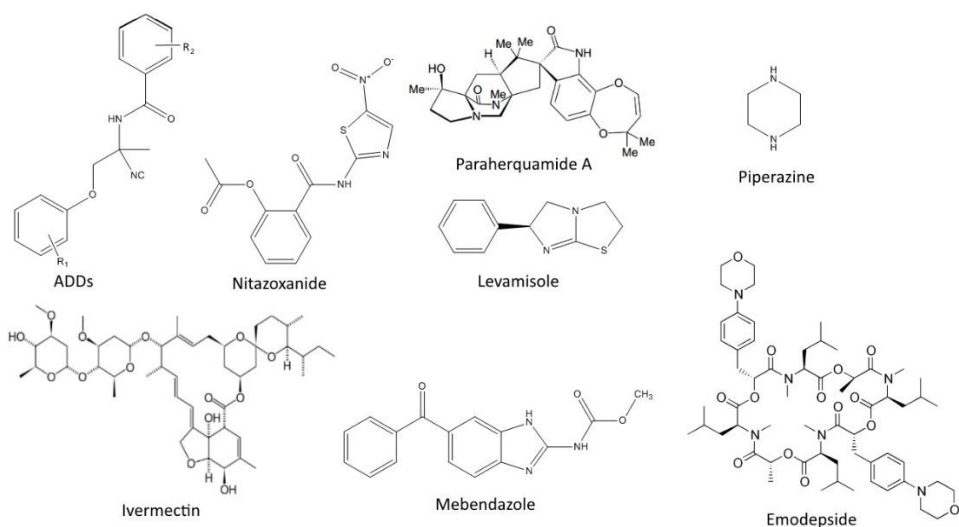


Figure 2. Examples of different anthelmintic drugs. Created by Josh Foster.

Due to the developing resistance to anthelmintic drugs in *H. contortus*, a novel drug candidate must be discovered to manage the spread of haemonchosis, as well as treatment options for other infected animals. Certain ligand-gated ion channels (LGICs) may be potential targets for new anthelmintic drug candidates.

5. Ligand-Gated Ion Channels

Ligand-gated Ion Channels (LGIC) play key roles in the nervous system. The binding of specific neurotransmitters at synapses in the nervous system causes activation of these receptors triggering a reaction in the postsynaptic membrane allowing for anions or cations to enter into the postsynaptic cell (Nys et al., 2013). The binding of the neurotransmitter ligand causes a conformational change which opens the channel and allows ions to flow through due to their electrochemical gradients. This only occurs for a short duration of time (milliseconds), but the flow of ions is great enough to cause a rapid response (Unwin, 1993). Many of these LGICs are composed of five subunits located in the cell membrane forming a channel. Many LGICs are heteromultimers with many genes encoding the different subunits. This allows for a large diversity between receptors giving many different characteristics such as pharmacological and biophysical properties, expression patterns within tissue and between different kinds of tissue (Alexander et al., 2011).

Cysteine-loop LGICs (cys-loop LGIC) are pentameric neurotransmitter receptor channels that function in the central and peripheral nervous system. These channels have been found throughout vertebrates, invertebrates and prokaryotes, and have homologous structures and similar mechanisms of action (Thompson et al, 2010). These receptors are the targets of many pharmaceutical drugs as well as pesticides. Each subunit of the cys-loop LGIC is composed of an extracellular N-terminus with a ligand binding site as well as a 13-amino acid loop which

contains two cysteine residues forming a disulfide bond (Connolly et al., 2004; Thompson et al, 2010). The pentameric channel can be composed of a variety of subunits arranged pseudo-symmetrically around a central pore (Thompson et al, 2010) (Figure 3). This pore allows for anions or cations to flow with their electrochemical gradient either into or out of the cell. The extracellular domains (ECD) of the cys-loop LGIC have been difficult to model and so, until recently, the acetylcholine binding protein was used as a model due to its homology to cys-loop receptors (Thompson et al, 2010). The ligand binding site occurs between two adjacent subunits and is found between 3 loops (A, B and C) of the principal subunit, and three β -sheet 'loops' (D, E and F) of the complimentary subunit (Thompson et al, 2010). These loops contain aromatic residues which form cation- π interactions with the natural ligand. There are four transmembrane domains (TMD), M1 through M4, in each subunit of the cys-loop receptor (Figure 3.) The M2 regions of each subunit line the central pore and are responsible for the selectivity of the ions flowing through the channel (Thompson et al, 2010; Connolly et al., 2004) while the M1, M3 and M4 shield the channel from the lipid surroundings. M2 has specific functions in channel gating and opening, and bridges the ECD and the TMD, which involves a transmission of energy from ligand binding into channel opening (Thompson et al, 2010). The movement of the ECD as well as the M2-M3 linker on the extracellular side destabilizes a hydrophobic region moving it away from the central pore and allowing for the channel to open. While some receptors show salt-bridges connecting the ECD and TMD, it is postulated that others maintain a global electrostatic attraction instead (Thompson et al., 2010). It has been shown that M1, M2 and M3 maintain position within the membrane while M4 is less restrained (Thompson et al, 2010). M3 and M4 have an intracellular loop which can be described as a 'hanging-basket' type structure which

characterizes the intercellular domain (ICD) and is involved in the positioning of the channel within the membrane (Thompson et al, 2010).

The structural and functional homology of cys-loop receptors allows for comparison of channels amongst many different species, from vertebrates to invertebrates. In vertebrates, excitatory channels are cationic and include both serotonin-gated channels and acetylcholine-gated channels. Inhibitory channels are anionic and include both GABA_A and glycine-gated channels. Invertebrates have far more numerous LGIC which include channels activated by histamine, glutamate, acetylcholine, serotonin, dopamine, and tyramine. Interestingly, excitatory GABA receptors have been identified in invertebrates (Schuske et al., 2004).

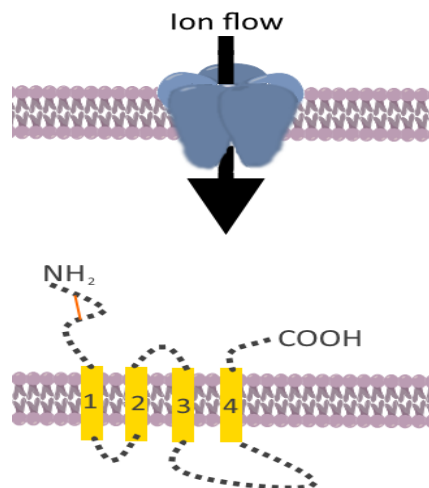


Figure 3. Representation of the pentameric channel with ion flow direction (top). The individual subunit can be seen represented with the 4 transmembrane domains 1 through 4. The orange line represents the disulfide bond of the cys-loop (bottom). Created by Josh Foster

5.1 GABA receptors

In vertebrates neurotransmission can result in both excitatory and inhibitory functions. This is dependent on a balance between excitatory and inhibitory neurotransmitters. If there is an

overabundance in excitatory neurotransmission it will result in epileptic seizures, whereas an overabundance of inhibitory neurotransmission will result in loss of consciousness (Schuske et al., 2004). The primary inhibitory neurotransmitter in vertebrates is GABA (Figure 4) (Alexander et al, 2011). The inhibition caused by GABA occurs when the neurotransmitter binds to a

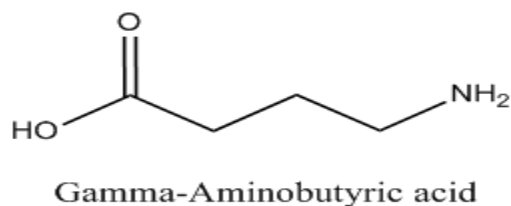


Figure 4. Chemical structure of Gamma-Aminobutyric acid (GABA). Created by Josh Foster

variety of different membrane-bound GABA receptors (Alexander et al., 2011). These include both metabotropic receptors that are G-protein coupled receptors (GABA_B), as well as ionotropic ligand-gated ion channels (GABA_A and GABA_C). GABA_A and GABA_C are both GABA-gated chloride channels which, when opened, allow for the influx of chloride ions into neurons, inhibiting neuronal firing (Alexander et al., 2011).

Mammalian GABA_A receptors are composed of five subunits which assemble to form a pentameric channel. These subunits are encoded by 19 different genes. However, most physiological heteromers are theorized to include two α subunits, two β subunits, and one γ subunit. It is also found that the β 3 subunit is capable of forming functional homomeric channels (Miller et al, 2014; Saras et al, 2008). The GABA molecule acts as a neurotransmitter and binds to the extracellular domain at the α/β subunit interface causing a conformational change which causes the transmembrane region to open the ion channel (Sigel et al., 2012). Recently, Miller et

al (2014) crystalized the $\beta 3$ homopentamer channel (Figure 5), which shed light on the structural information that was previously unavailable. It was found that the GABA_AR- $\beta 3$ subunits form the most energetically favorable interactions between ECDs by utilizing patches of hydrogen bonds, salt bridges and van der Waals forces.

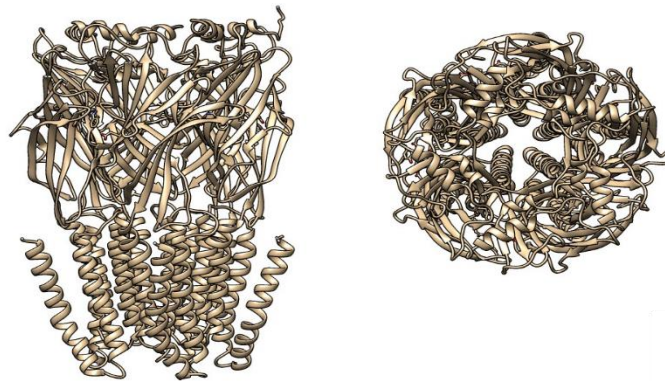


Figure 5. Left: Side view of the crystal structure of human GABA_A- $\beta 3$ channel. Right: Top-down view of the GABA_A- $\beta 3$ channel. PDB 4COF (Miller et al., 2014)

Activation of the GABA_A receptor requires key molecular components of adjacent subunits in the extracellular loops which comprise the binding site for GABA (Accardi et al., 2011). The aromatic box of loops A to D directly bind to GABA (Accardi et al., 2011) or stabilize the binding pocket (Accardi et al., 2011). These residues include $\beta 2Y97$ of loop A, $\beta 2Y157$ of loop B, $\beta 2Y205$ of loop C and $\alpha 1F64$ of loop D (Accardi et al., 2011).

5.2 GABA receptors in nematodes

While GABA is only inhibitory in vertebrate organisms, it can also be excitatory in invertebrates (Schuske et al., 2004; Accardi et al, 2012). In nematodes, GABA is used both as an inhibitory neurotransmitter, allowing for locomotion by relaxing muscles on one side of the body

while contraction occurs on the other, as well as an excitatory neurotransmitter in expulsion of intestinal contents (Schuske et al., 2004). In nematodes the primary inhibitory GABA receptor is UNC-49. *Caenorhabditis elegans* has been found to express three UNC-49 subunits including Cel-UNC-49A, Cel-UNC-49B and Cel-UNC-49C (Bamber et al., 1999). These subunits are encoded by a single gene, *unc-49*, which undergoes alternative splicing and forms different functional channels (Bamber et al., 1999). These channels maintain similar N-terminal ligand binding domains, but vary in their C-terminus. While it is possible for Cel-UNC-49B to form homomeric channels, it appears as though the Cel-UNC-49B/C heteromeric channel is the native channel in *C. elegans* (Bamber et al., 1999). The Cel-UNC-49A subunit does not appear to be expressed in physiologically significant levels (Bamber et al., 1999). The heteromeric Cel-UNC-49B/C channel plays a role in locomotion and is expressed at neuromuscular junctions (Bamber et al., 1999). Relative to the Cel-UNC-49B homomeric channel, the heteromeric Cel-UNC-49B/C shows decreased sensitivity to GABA as well as altered responses to both modulators and inhibitors which indicates functional differences between the two subunits (Bamber et al., 2005). While UNC-49 receptors share a relation with vertebrate receptors, they also show pharmacological differences, such as the insensitivity to bicuculline, and altered responses to the enhancing effects of benzodiazepine (Bamber et al., 2005). Bamber et al., (1999) found that these subunits are not actual orthologues of the GABA_A receptors found in vertebrates, but they do share functional and structural overlap suggesting conservation within GABA receptor families.

5.3 GABA receptors in *H. contortus*

The function of GABA reception in parasitic nematodes is less understood relative to *C. elegans*. There are two gene orthologues of the *unc-49* subunits in *H. contortus*. These include

unc-49B and *unc-49C* (Siddiqui et al., 2010). There are many shared functional characteristics between the *C. elegans* and *H. contortus* UNC-49B and C proteins. However, the Hco-UNC-49B receptor (Figure 6) shows some key functional differences (Siddiqui et al., 2010). It is interesting to note that while the heteromeric channel in *C. elegans* shows decreased sensitivity to GABA, it is the Hco-UNC-49B homomeric channel (not the heteromeric channel) that shows decreased sensitivity in *H. contortus* (Siddiqui et al., 2010). For example, Siddiqui et al., 2010 showed that co-expressing the Cel-UNC-49B subunit with Hco-UNC-49C subunits demonstrates a decreased sensitivity to GABA which is consistent with the *C. elegans* heteromeric channels. When the expression is reversed (i.e., expressing Hco-UNC-49B and Cel-UNC-49C), there is a higher sensitivity to GABA which indicates that the Hco-UNC-49B subunit of *H. contortus* increases GABA sensitivity. The cause of the increased sensitivity is unknown, although differences in the length of the intracellular loops (M3-M4) between *C. elegans* and *H. contortus* have been detected. Also, the homomeric channel is more sensitive to the channel blocker picrotoxin, which indicates that the picrotoxin resistance can be attributed to the Hco-UNC-49C subunit of the heteromeric channel (Siddiqui et al., 2010)

While the mammalian GABA_A receptor may not be an actual orthologue of the UNC-49 proteins, it has been found that N-terminus of UNC-49B shares 69% and 73% sequence similarity to the $\alpha 1$ and $\beta 2$ subunits, respectively. Many residues of the discontinuous loops A through F are conserved, including the residues of the aromatic box which forms the binding site. Accardi et al., (2011) found that the specific residues of the aromatic box of the mammalian GABA_A receptor ($\alpha 1$ F64 of loop D, $\beta 2$ Y97 of loop A, $\beta 2$ Y157 of loop B, and $\beta 2$ Y205 of loop C) is functionally conserved in Hco-UNC-49B as Y85, F127, Y187 and Y239. Mutations of these residues substantially impact the function of Hco-UNC-49 channels.

Although there are many similarities between *C. elegans* and *H. contortus* GABA receptors, as well as some functional similarities with the mammalian GABA_A receptor, further molecular studies are needed to better understand the function of GABA neurotransmission in parasitic nematodes. Some amino acid residues that may play an important role in the function of the UNC-49 receptor of *H. contortus* include residues that have a charge. As stated above charged residues can play key roles in the formation of the structure of this channel (through salt bridge interactions) and its interaction with ligands.



Figure 6. Model representative of the *Haemonchus contortus* UNC-49B homomeric channel with the 6 loops represented on the primary (A-C) and complimentary subunits (D-F). Created by Micah Callanan.

Modelling of the UNC-49 receptor of *H. contortus* and observation of conserved regions of other LGIC, reveal locations which may serve as salt bridges (Figures 7 and 8). Two sets of residues which may be considered as potential for salt bridges in *H. contortus* include D83-H137 or R159 and R241-E185. Interestingly, the crystal structure of the Human GABA_A receptor shows similar salt bridges at these locations, and a series of bridges crossing E155-R207-E153-K196 (Miller et al., 2014; Bergmann et al., 2013) which are equivalent to Hco-UNC-49B's E185-R241-E183. In order to further understand the function of these residues a series of point mutations were introduced and examined using two-electrode voltage clamp electrophysiology.

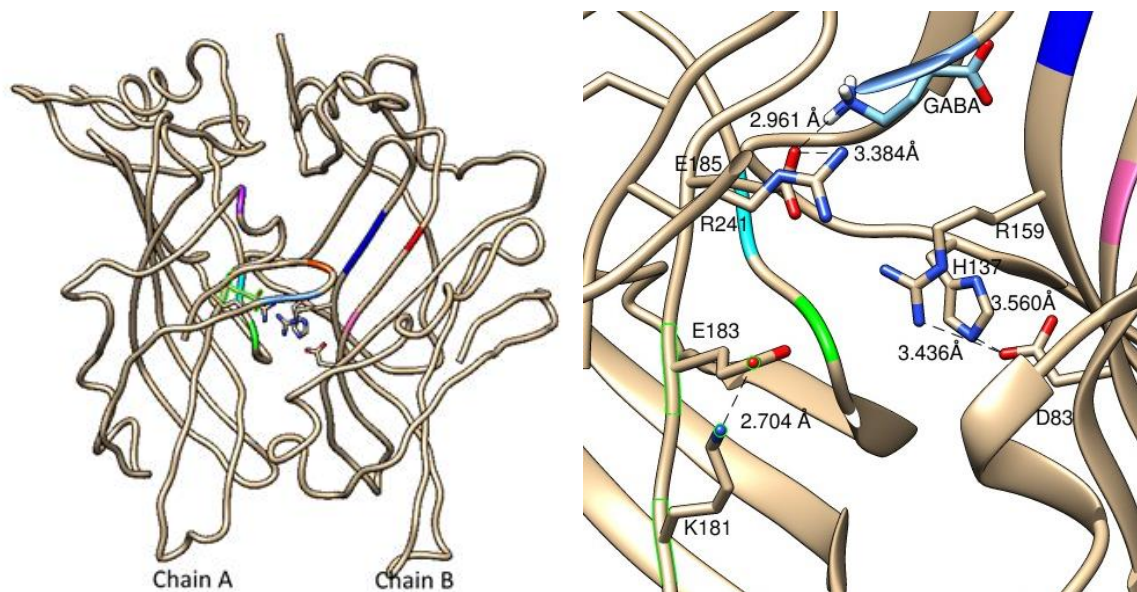


Figure 7. Left: Residues for the proposed salt bridges shown in relation to their positions on both the primary (chain A) and complimentary subunits (Chain B) Right: Close up of the proposed salt bridges with distances and labelling of the residues. Created by Micah Callanan.

Materials and Methods

6. Methods

6.1. UNC-49B mutant primer design

The amino acid sequence of Hco-UNC-49B (GenBank Accession # EU939734.1) was aligned with other ligand-gated chloride channels (LGCC) such as GABA_c rho-1, GABA_A α 1, Cel-UNC-49B, and AChBP, (shown in Figure 8). These were used to determine conserved charged amino acids and were compared to a premade model of our receptor that used *C. elegans* GluCl as a template (Kaji et al., 2015) to determine distance between charged residues. If the residues were $\sim 4.0\text{\AA}$ they were considered for further examination. Fifteen mutants were generated using Stratagene's web-based QuikChange® Primer Design program (www.stratagene.com/sdmdesigner/default.aspx). These mutants are summarized with the pair of mutagenic primers in the appendices (Table 1). Each set of mutants were designed to mutate each half of the salt-bridge to an alanine to remove salt bridge function, then to a similarly charged residue to mimic function, and then to a residue swap to attempt to rescue function. Based on the sequence of the Human GABA_A β 3 receptor, D83T was created to compare Hco-UNC-49B/C to the functional GABA_A β 3 homomeric mammalian channel (which naturally contains a threonine in the analogous position).

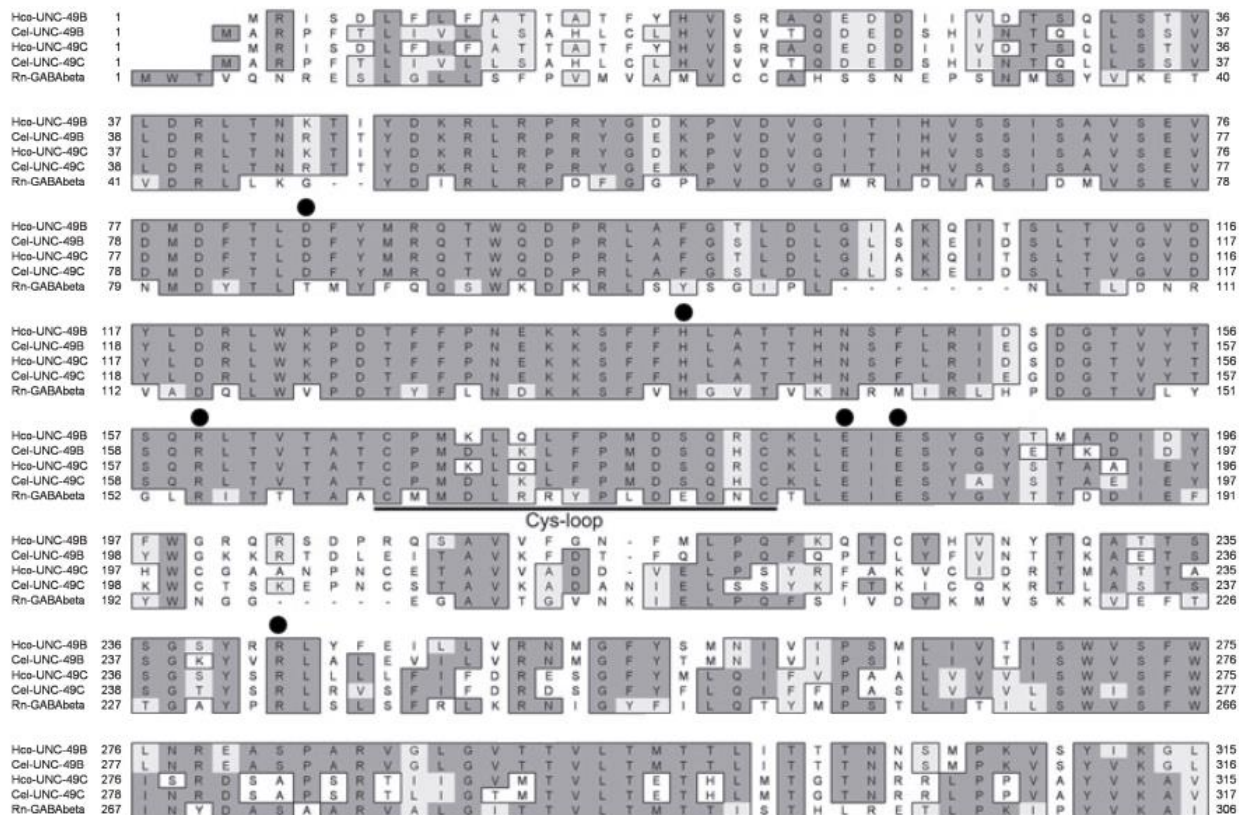


Figure 8. Sequence comparison of Hco-UNC-49B with other LGIC for the determination of charged residues.

6.2. cRNA production of UNC49B mutants

mRNA provided by McGill university was used to produce the coding sequence of UNC49B and subcloned into the pT7TS vector with an untranslated *X. laevis* beta-globin gene (Figure 9). Mutations were introduced using the QuikChange II site directed mutagenesis kit and transformed into supercompetent cells and verified by sequencing at McGill University. cRNA was produced by *in vitro* transcription using T7 RNA polymerase and precipitated using lithium chloride and resuspended in H₂O.

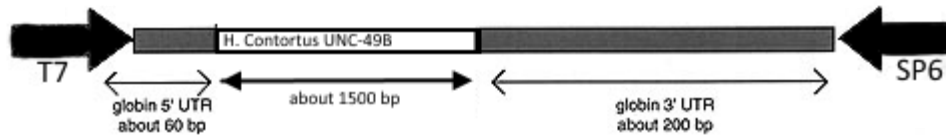


Figure 9. pT7T5 vector with *H. contortus unc49* insertion. Created by Josh Foster

6.3. Expression of *UNC49B* mutants in *X. laevis* oocyte

Xenopus laevis were anesthetized using 0.15% 3-aminobenzoic acid ethyl ester, methanesulphate salt buffered to pH 7 with sodium bicarbonate. Oocytes were surgically removed and cut into small clumps of approximately 20 eggs per clump. These were incubated in OR-2 (82mM NaCl, 2mM KCl, 1mM MgCl₂, 5mM HEPES, pH 7.5) with type-II collagenase for 2 hours while shaking. These were then placed in ND96 supplemented with pyruvate and gentamycin. Oocytes were injected with 50 nL of either wild-type, or mutant Hco-UNC-49B cRNA, and wild type Hco-UNC-49C using the Drummond Nanoject microinjector. These are stored at 20°C for one day, replacing the supplemented ND96 twice before electrophysiology.

6.4. Two-electrode voltage clamp electrophysiology

Approximately forty-eight hours after injection, electrophysiology was performed using the Axoclamp 900A voltage clamp. Responses were recorded using varying concentrations of GABA dissolved in non-supplemented ND96. Microelectrodes were made using Ag|AgCl wires and filled with 3M KCl. Injected *X. laevis* oocytes were clamped and held at -60mV and left for 1-2 minutes to stabilize before GABA was washed over the oocytes. Figure 10 illustrates the electrophysiology set up and theory. Data was recorded and analyzed using Clampex 10.3 software and graphs were produced using Graphpad Prism Software 5.0. Data was collected

from at least four individual oocytes. To assure consistency, two different batches of oocytes were used. Dose-response curves are fitted to the equation:

$$I_{max} = \frac{1}{(1 + (EC_{50}/[D])^h)}$$

Where I_{max} = the maximal response, $[D]$ is the concentration of the drug, EC_{50} is the concentration of the drug producing a half-maximal response and h is the Hill coefficient.

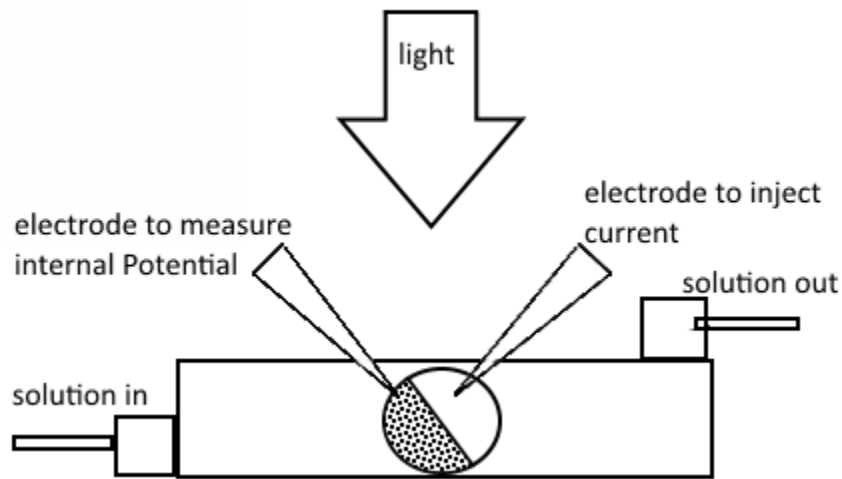


Figure 10. Two-electrode voltage clamp electrophysiology set up with GABA and ND96 as the solution in and the waste solution out. Created by Josh Foster.

6.5. Modelling

Homomeric channel models were generated using Modeller software (Webb et al., 2014) with the *C. elegans* GluCl channel as a template. Molecular graphics and analyses were performed with the UCSF Chimera package. Chimera is developed by the Resource for

Biocomputing, Visualization, and Informatics at the University of California, San Francisco
(supported by NIGMS P41-GM103311).

6.6. Substituted Cysteine Accessibility Method

Cysteine Accessibility was determined for Hco-UNC-49B R159C using the methanethiosulfonate (MTS) agent 2-hydroxyethylthiosulfonate (MSET) obtained from Toronto Research Chemicals (Toronto, ON, CA). Each oocyte was washed and subjected to their predetermined EC_{50} concentration of GABA after response stabilization by multiple hits with GABA. Once stabilization of responses was determined, MSET (1mM for 1 min) was perfused over the oocyte followed by 5 min wash with ND96 solution. EC_{50} of the mutant was then reapplied and currents were recorded.

Results

7. Results

7.1. Electrophysiology of mutants

Amino acids were chosen based on their charge and proximity to other charged amino acids with the prediction that these residues would form salt bridges within the subunit of Hco-UNC-49B. In order to assess the accuracy of this prediction, electrophysiology was performed using TEVC. Mutants were generated to test the participation in a potential salt bridge by first removing the amino acid while retaining its place by substitution with alanine. The second mutation tested whether the conservation of charge would rescue receptor function. In these mutations each residue was substituted with a residue of equal charge. Finally, swap mutations were generated by mutating both residues of the salt bridges to the opposite residue. Each mutated receptor was exposed to GABA in increasing concentrations to determine the EC₅₀ in order to determine the effect each residue have on function. Upon recording, it was found that most receptors with mutated subunits showed some sort of activity, and clean tracings were established for comparisons and determination of EC₅₀ (Table 1). While most receptors were functional, D83A, R159K, and all mutations at position E185 showed no responses to GABA at concentrations less than 20mM.

Table 1. Charged residue mutations of potential salt bridges. EC₅₀ are compared for the heteromeric UNC-49B/C receptor with GABA.

Mutation	EC₅₀ ± S.E. (μM)	Number of oocytes
Wild-Type	68.03±17.3	6
D83A	n.r. <20,000	10
D83E	276.1 ± 36.99	5
D83T	519.7 ± 39.72	5
H137A	2174 ± 173.3	5
H137K	4166 ± 744.74	5
R159A	5469± 395.72	7
R159K	n.r. <20,000	11
E183A	735.2 ± 131.48	6
E185A	n.r. <20,000	13
E185D	n.r. <20,000	5
R241A	5174 ± 472.5	6
R241K	3793 ± 435.4	6
D83H/H137D	1315 ±140.42	5
D83R/R159D	598.5 ± 77.09	7
E185R/R241E	n.r. < 20,000	6

7.2. D83 mutations

Based on the model created with the *C. elegans*' GluCl receptor as a template, D83 was predicted to be in close enough proximity with both R159 as well as H137 to form a salt bridge (3.560Å and 3.436Å respectively). Mutations of D83 were conducted to assess its importance as a potential salt bridge residue. It was found that D83A showed a complete knock-out of function with an EC₅₀ greater than 20mM (n=10). Conservation of the charge through D83E mutation showed a drastically rescued function with an EC₅₀ of 276.1uM, an approximately 4 fold decrease in sensitivity relative to the wild-type channel (n=5). Finally, to determine the importance of charge versus polarity, a D83T mutation was assessed and found to have an EC₅₀ of 519.7uM, an approximately 8 fold decrease in sensitivity (n=5). To compare these mutations, dose response curves were determined (Figure 11).

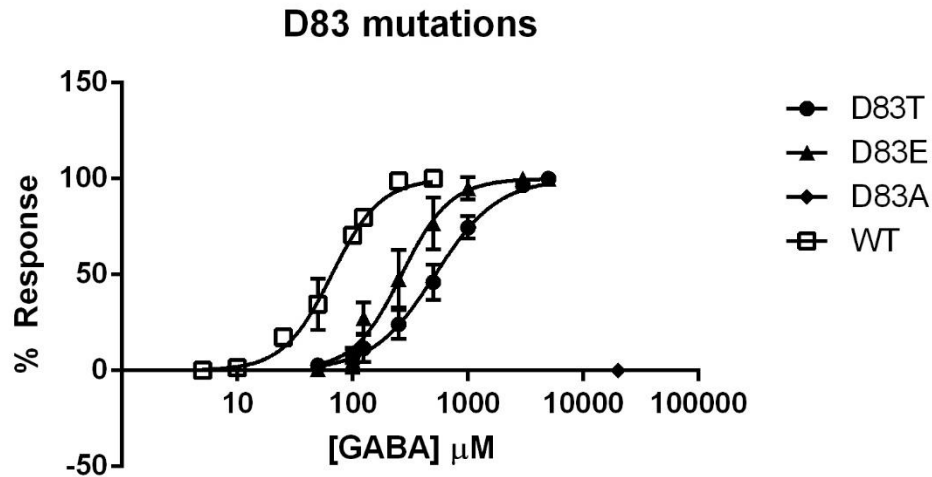


Figure 11. Dose response curves of D83 mutations.

7.3. H137 mutations

In order to effectively determine whether the D83 residue is forming a salt bridge with H137, a number of mutations were analyzed. Firstly, an H137A mutation was created and was found to have an EC_{50} of $2174\mu\text{M}$ for GABA, an approximately 34 fold decrease in sensitivity ($n=5$). In order to attempt to rescue the receptor function, a similarly charged residue was substituted in H137K. It was found that despite the charge conservation there was an EC_{50} of $4166\mu\text{M}$, an approximately 65 fold decrease in sensitivity ($n=5$). This demonstrates that the H137K is less sensitive to GABA compared to H137A despite the conservation of charge, and in both cases a mutation at this position drastically hindered the receptor's function. To compare these mutations, dose response curves were determined (Figure 12).

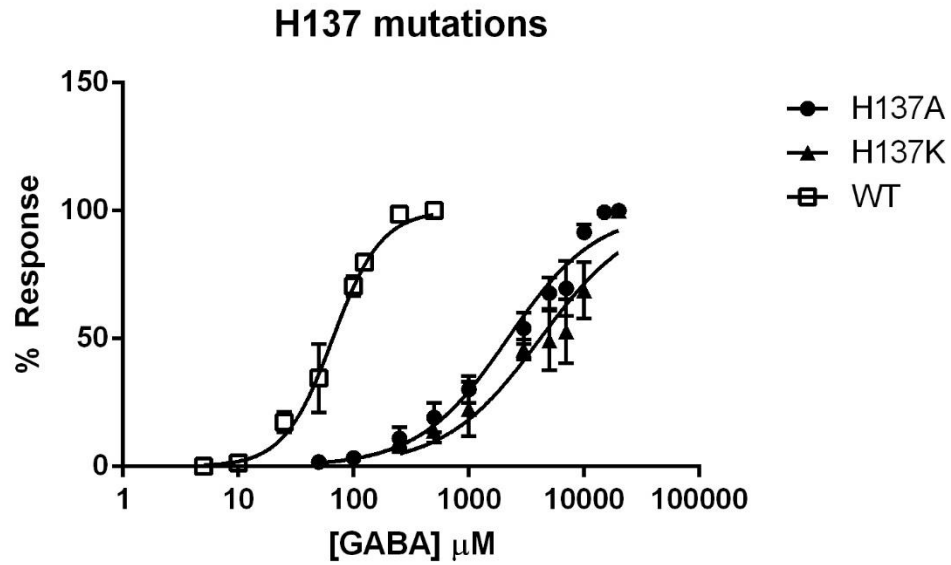


Figure 12. Dose response curves of H137 mutations.

7.4. R159 mutations

The other potential half of the D83 salt bridge is R159. In order to evaluate its participation in this salt bridge, the same two mutations were implemented. To test the removal of R159, an R159A mutant was generated and analyzed through determination of the EC_{50} for GABA. It was found that R159A had an EC_{50} of $5469\mu\text{M}$, an approximately 93 fold decrease in sensitivity ($n=4$). Again, to determine if conservation of charge could rescue receptor function, an R159K mutant was generated. However, despite conservation of charge, R159K showed no response to GABA at concentrations less than 20mM ($n=11$). To compare these mutations, dose response curves were determined (Figure 13).

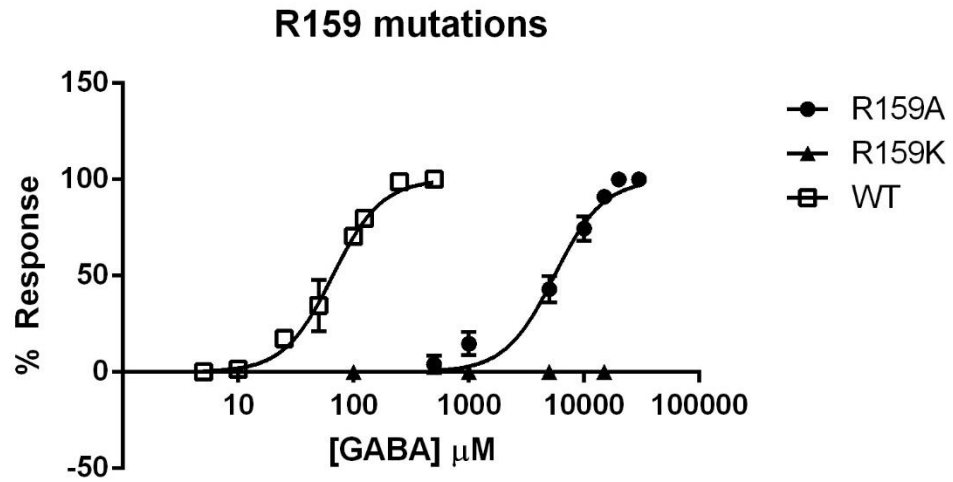


Figure 13. Dose response curves of R159 mutations.

As an additional examination of R159 an R159C mutation was examined using the reducing agent MTSET. It is well known that MTSET will covalently bind to cysteines which will affect the function of the channel. The effect can be seen using electrophysiology. Here the addition of MTSET caused the GABA response (measured as a current) to increase by 25% (Figure 14).

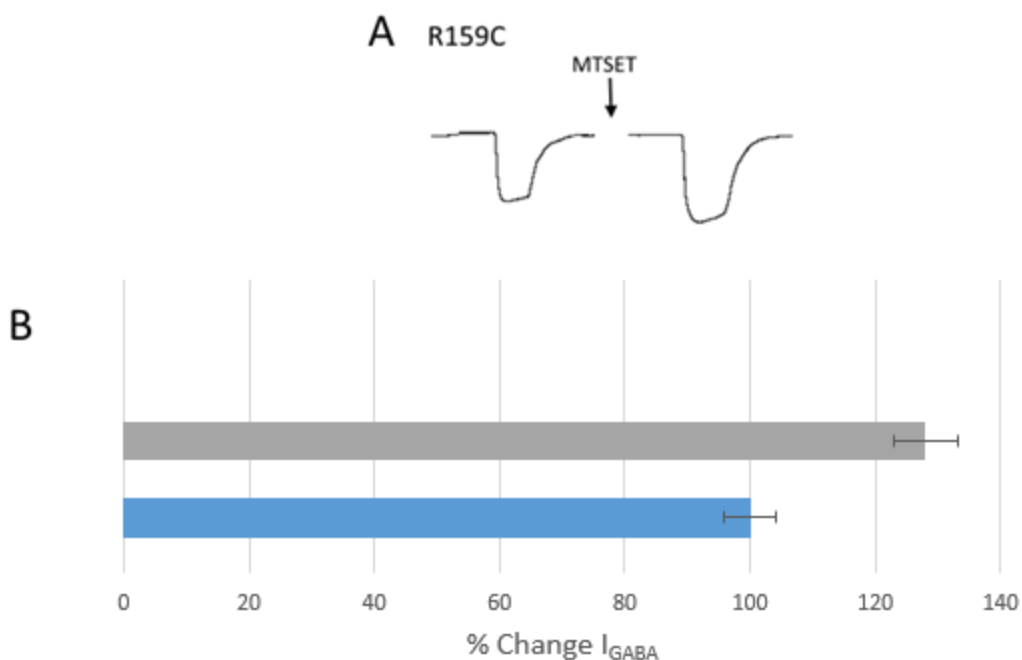


Figure 14. Results of experimentation with MTSET on R159C mutant. Blue bar is the current before MTSET. Grey bar is after the addition of MTSET.

7.5. E183 mutations

Based on the *C elegans* GluCl template model that was generated, E183 is in close proximity to K181 and potentially forms a salt bridge with this residue (2.704 Å). In order to determine the possible function of this residue in participation as a salt bridge, an E183A mutant was generated. E183A showed an EC_{50} of 735.2 μ M, an approximately 19 fold decrease in sensitivity relative to the wild-type EC_{50} (n=6). To compare this mutation with wild-type, dose response curves were determined (Figure 15).

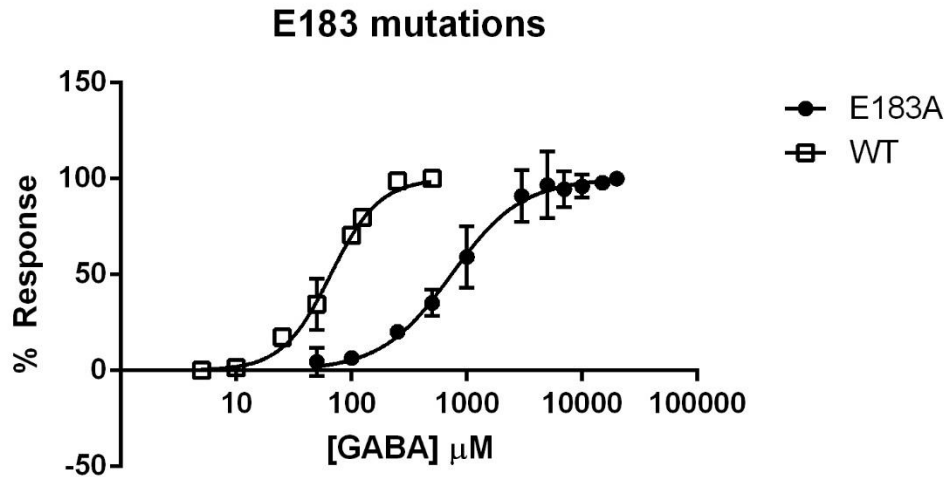


Figure 15. Dose response curves of E183 mutations.

7.6. E185 mutations

E185 is in close proximity to R241 of loop C (3.384Å) allowing it to potentially form a salt bridge with the residue. Mutations of E185 to both alanine as well as the similarly charged aspartic acid yielded a complete loss of function of the channel with no responses to GABA at concentrations less than 20mM (Table 1).

7.7. R241 mutations

Finally, in order to test the potential E185/R241 salt bridge, mutants were generated for R241 as described previously. It was found that the mutation R241A showed an EC_{50} of 5174 μM , an approximately 80 fold decrease in sensitivity relative to wild-type (n=6). The R241K mutation showed a small increase in sensitivity to GABA with an EC_{50} of 3793 μM , an approximately 59 fold decrease in sensitivity relative to wildtype (n=6). Both mutations showed a drastic hindrance to the receptors function. To compare these mutations, dose response curves were determined (Figure 16).

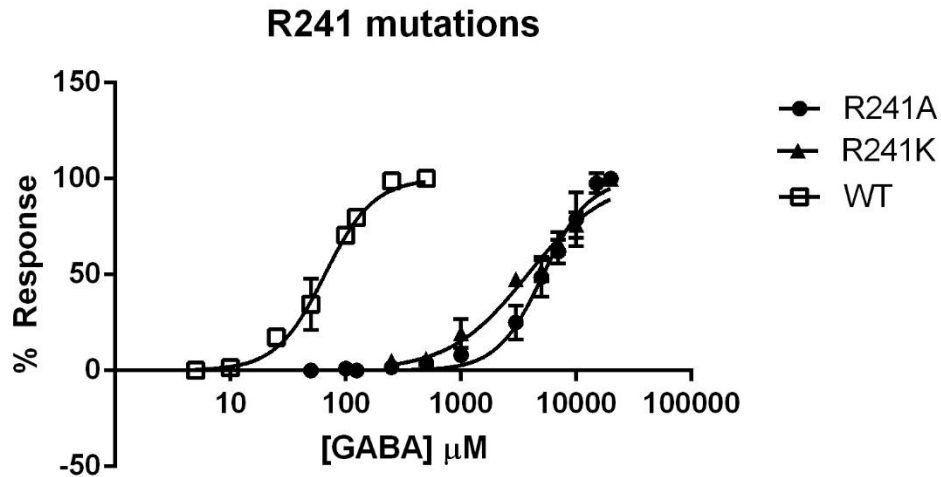


Figure 16. Dose response curves of R1241 mutations.

7.8. Swap mutations

The final mutations generated to determine salt bridges are described as swap mutations. This utilized two mutations in each subunit to generate mutants with the two residues swapped. This generated the mutants D83H/H137D, D83R/R159D and finally E185R/R241E. The D83H/H137D mutation yielded an EC_{50} of 1315 ± 140.4235 , an approximately 39 fold decrease in sensitivity relative to wild type (n=5). The D83R/R159D mutant showed an EC_{50} of 598 ± 77.0919 , an approximately 9 fold decrease in sensitivity relative to wild type (n=7). The final swap mutation, E185R/R241E showed no response less than 20mM (n=6) (Figure 17).

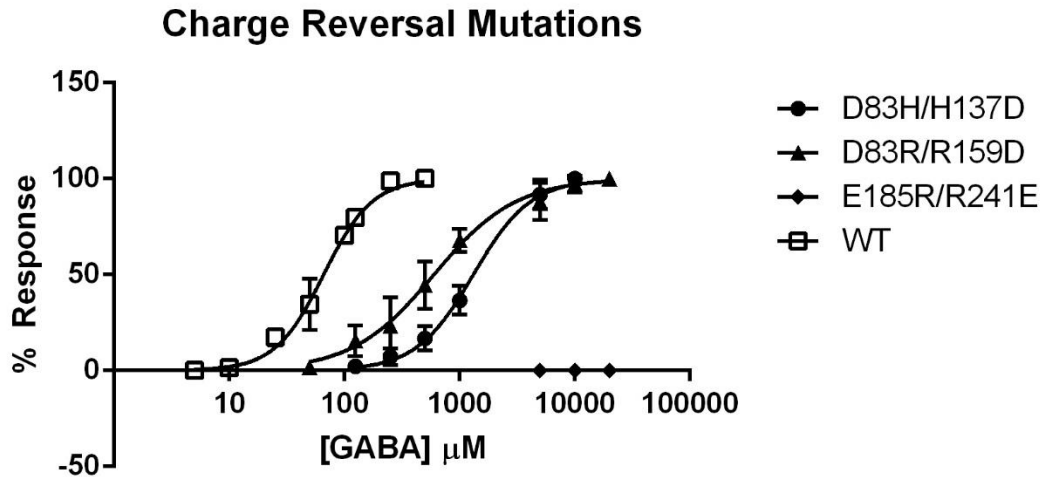


Figure 17. Dose response curves of charge reversal mutations.

7.9. Modelling results

A model of the binding site of Hco-UNC-49B homodimer was generated using the *C. elegans* glutamate gated chloride channel (GluCl) as a template. This model has been used for determining the proximity and orientation of residues for the potential salt bridges of Hco-UNC-49B. The distances of the chosen residues (D83, H137, R159, K181, E183, E185 and R241) are found in Table 2 and in Figure 18. How the model corresponds to the electrophysiology results is examined in the discussion.

Table 2.
Distances between residues of the predicted salt-bridges of UNC-49B.

Interacting Residues	Distance
D83-H137	3.560Å
D83-R159	3.436Å
E185-R241	3.384Å
E185-GABA	2.961 Å
K181-E183	2.704 Å

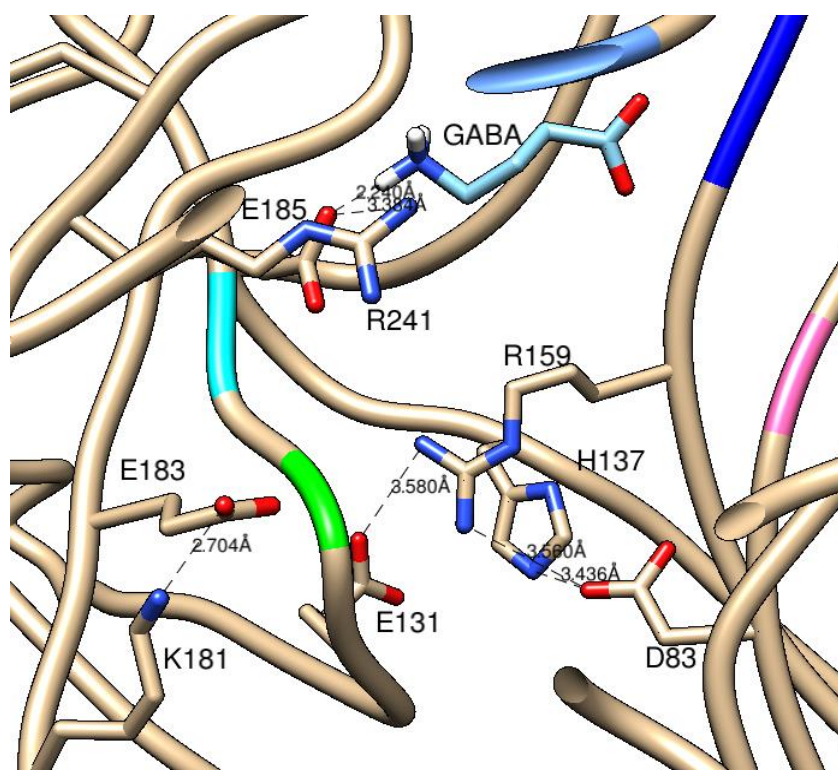


Figure 18. Close up of the relevant residues for the proposed salt bridges with distances and labelling of the residues. Model created by Micah Callanan

Discussion

8. Discussion

Many articles have addressed the importance of salt bridges in LGIC and their role in both ligand interactions and positioning of subunit loops (Bosshard et al., 2004). While these articles address familiar organisms such as *C. elegans* (Siddiqui et al., 2010), *D. melanogaster* (Ashby et al., 2012), and humans (Bergmann et al., 2013), this thesis was composed to look at the unique GABA receptor, Hco-UNC-49. Utilizing sequence homology and a model generated using the *C. elegans* GluCl channel as a template, four potential salt bridges were chosen. In order to investigate these potential salt bridges and their functions, a series of mutations were generated and analyzed through electrophysiology.

8.1. Salt-bridges

Throughout this study, four potential salt bridges were investigated. These salt bridges included a potential bridge between D83-H137, D83-R159, E185-R241 and K181-E183. It has previously been shown that there is a salt bridge critical to receptor function between the analogous residues of E185 and R241 in both *D. melanogaster*'s RDL receptor (Ashby et al., 2012), as well as the Human GABA_A receptor (Newell et al., 2004; Bergmann et al., 2013). The analogous residues of E185 (E155 in GABA_A, E204 in RDL) and R241 (R207 in GABA_A, R256 in RDL) have both been shown to be crucial for the activation of the channel in the RDL receptor as well as GABA_A (Ashby et al., 2012; Miller et al., 2014; Newell et al., 2004). It has been suggested that E155 acts as a control element involved in coupling the binding of ligands to the channel activation (Newell et al., 2004), and that mutations of R207 affects GABA binding and unbinding rates (Bergmann et al., 2013). Utilizing an agonist binding model, E155 is flanked by R207 and allows for an electrostatic interaction between R207 and GABA as E155 is at a correct

distance to form a salt bridge with GABA deep in the binding pocket (Bergmann et al., 2013). Finally, crystallography has revealed that the analogous residues of the GABA_A receptor are in fact a salt bridge (Miller et al., 2014). Interestingly, the analogous residue of E183 (i.e., E153 in GABA_A) has been shown to form a salt bridge to a loop C residue (K196 in GABA_A) which is not present in Hco-UNC-49B. It is also speculated that E153 is in close proximity to E155 and R207 and may be a part of a larger network of interacting residues (Venkatachalan et al., 2008; Newell et al., 2004). The crystal structure also demonstrates that a closed conformation of the channel is stabilized by salt bridges between E155-R207-E153 (Miller et al., 2014) which further supports the notion that there is a larger network of bridges present. Our results demonstrate that like the GABA receptor in both *Drosophila* and human, the analogous residues E183, E185 and R241 are all important for receptor function. However, while E183 may be important it may not have an identical function in Hco-UNC-49 compared to its role in the human GABA_A receptor.

Literature supports the results of this thesis (Ashby et al., 2012) in that, all mutations to the analogous residue of E185 (in the RDL receptor) resulted in channels that were unresponsive. The model of Hco-UNC-49 demonstrated a distance between E185 and R241 of 3.394Å. This is close enough to form a salt bridge. Furthermore, in the model, the distance between E185 and the protonated amine of GABA is 2.961Å. This explains why mutations of E185 results in unresponsive channels, as E185 is crucial for the binding of GABA and allows for the electrostatic interaction from GABA to R241 of loop C. Mutations of R241 also showed drastically impaired function of the channel, with R241A showing an approximately 80 fold decrease in sensitivity and R241K showing an approximately 59 fold decrease in sensitivity.

Despite the positioning of E185 relative to GABA and R241, it was previously discussed that there may be a network of salt bridges from E185-R241-E183 (Miller et al., 2014). The

guanidinium cap of arginine allows for interactions with both E185 as well as E183, whereas the lysyl side chain of lysine can only permit one interaction. Consistent with this, the R241K mutation showed a 59 % decrease in GABA sensitivity clearly demonstrating that the preferred residue is an arginine. It is possible that based on the chemistry and large side chain of lysine the salt bridge between E183 and R241K would be broken. This is supported by the results of the experimentation examining the RDL receptor which demonstrated no response to GABA when the R241 analogous residue was mutated to alanine or lysine (Ashby et al., 2012). The final set of mutations used to investigate the E185-R241 salt bridge utilized a swap mutation, E185R-R241E. This produced a non-functional receptor which was likely caused by removal of critically important E185 which likely also interacts with GABA, as indicated by others (Bergmann et al., 2013; Newell et al., 2004).

As previously described, E183 may form a salt bridge with K181 and possibly R241 (Venkatachalan et al., 2008). However, the model of Hco-UNC-49 showed a distance too great between R241 and E183 to form a salt bridge, and thus only an interaction between E183 and K181 was investigated. Mutations of E183A showed a decreased sensitivity to GABA of ~19 fold relative to wild-type. This indicates that E183 is indeed important for receptor function. However, in order to further characterize the association of these residues, further analysis will be required.

Two other potential salt bridges were investigated. This included D83-H137 and D83-R159, as D83 is within reasonable proximity to form a salt bridge with both of these residues (3.560Å and 3.436Å, respectively). It has been shown that this histidine (H107 in GABA_A) regulates the Zn²⁺ inhibition in GABA_A receptors (Dunne et al., 2002). Mutations of H107A demonstrated non-functional channels in GABA_A (Dunne et al., 2002). Furthermore, mutations to either lysine

or arginine, both of which maintain the positive charge of histidine, showed non-responsive channels (Dunne et al., 2002). It has been suggested that H107 may not be important for assembly, folding or transport of the GABA_A receptor, but may be important for ion channel gating (Dunne et al., 2002). Crystal structures of the GABA_A channel show that H107 does in fact participate in ion selection and the flow of chloride ions (Miller et al., 2014). This is accomplished through interactions with other amino groups in positions 104 and 105 (Miller et al., 2014). Based on the literature for the GABA_A receptor, it could be concluded that H137 of Hco-UNC-49B does not participate in a salt bridge with D83. However, our electrophysiological results varied from the results demonstrated by Dunne et al., (2002). When the *H. contortus* H137A mutation was analyzed it was found to have an EC₅₀ of 2174μM for GABA, an approximately 34 fold decrease in sensitivity relative to wild-type. While this is a disruption in function for the channel, it still demonstrates a somewhat functional channel. The mutation H137K demonstrated an EC₅₀ of 4166μM, an approximately 65 fold decrease in sensitivity. This shows that despite the conservation of charge the receptor is still impaired.

The final mutation to test the potential salt bridge required a swap mutation of D83H-H137D. It was found that this mutant had an EC₅₀ of 1315uM. While this does demonstrate some rescue of function for the channel, it is still far from the wild type responses which suggests that this is not a salt bridge. However, further analysis would be required to determine if D83 and H137 are energetically linked.

D83 appears to be essential for receptor function as a mutation to an alanine produced a non-functional channel. Interestingly, a mutation which conserved the charge, D83E, showed a drastically improved EC₅₀ of 276.1uM. However, the GABA_A crystal structure showed the β3 homomeric channel to be functional despite the fact that an equivalent D83 is not present (the

analogous residue is T62) (Miller et al., 2014). In order to test whether or not a charged residue is required at this position in Hco-UNC-49B, D83T was analyzed. It was found that while it is not as sensitive as D83E, there is still a drastic improvement of function relative to the D83A mutant, with an EC₅₀ of 519.7uM. It should also be noted that while the GABA_A β3 homomeric channel is functional and lacks D83, the wild type channel is thought to be composed of a heteromeric channel including an α1 subunit which contains an aspartic acid at the equivalent position. With these results, there appears to be a unique nature to the D83 residue that has not previously been described in *H. contortus* or even human GABA receptors.

The research described here as well as research into other GABA receptors is consistent with the notion that there is some type of interaction between D83 and R159. For example, molecular simulations of the related invertebrate GABA receptor RDL has revealed a salt-bridge between D83 and R159. In the RDL, the analogous residue to R159 (which is R178) is located at the bottom of loop E where it forms an ionic interaction with D107, the equivalent to D83 in *H. contortus* (Ashby et al., 2012). In the present study when an R159A mutation was introduced the EC₅₀ increased to 5469uM. Likewise, R159K showed no response at concentrations less than 20mM. The final mutation generated to test the presence of a salt bridge was the D83-R159 swap. This mutation drastically rescued the function of the channel with an EC₅₀ of 598.5uM, albeit not as much as D83E. However, our model also suggests that R159 may also interact with E131 (Figure 18). Therefore, the swap mutation may disrupt this additional E131-R159 salt bridge, whereas the D83E mutation does not. It is still interesting though that D83T is relatively functional which suggests that the lack of charge at position 83 is tolerated. Again, further analysis is required to determine if D83 and R159 are energetically linked and the nature of this potential interaction. However, one experiment that points to a charge role of R159 is the

experiment using MTSET on a R159C mutant. When subjected to the compound MTSET, R159C shows an increased response to GABA. It has been suggested that an increased response with MTSET may be due to indirect effects of modifications and may alter gating or affinity for GABA (Boileau et al., 1999). It has also been suggested that MTSET may be utilized to predict the presence of salt bridges, as it has a positive charge (Venkatachalan et al., 2008). Experiments demonstrating an interaction between E153C and K196C of the human GABA_A receptor found that the use of MTSES and MTSET increased current amplitude in response to GABA (Venkatachalan et al., 2008). This supports the prediction that R159 may be interacting with either D83 or E131 as a salt bridge. While this is not conclusive evidence of a salt bridge, it does demonstrate the importance of these residues. Further research will be needed to determine the interaction that is occurring. Table 3 summarizes what is known about the interactions between residues in the human GABA_A receptor

Table 3. Summary of the comparison of residues between Hco-UNC-49B and the Human GABA_A receptors including the specific interactions found in GABA_A

Hco-UNC-49B	Human GABA_A	Specific Interaction in GABA_A	Reference
D83	α1D62, β3T62	Not determined	Boileau et al., 1999; Miller et al., 2014
H137	β3H107	Found to participate in ion selectivity	Miller et al., 2014
R159	β3R131	Salt bridges between β3R131-β3D101	Miller et al., 2014
E131	β3D101		
E183	β3E153	Salt bridge network from β3E155-β3R207- β3E155-β3K196	
E185	β3E155		
R241	β3R207		

Conclusion

9. Impact and conclusion

The objective of this thesis was to further characterize Hco-UNC-49B, the GABA receptor of *H. contortus*. This was accomplished by investigating four potential salt bridges found in conserved regions of Hco-UNC-49B. The amino acids which were thought to contribute to these salt bridges were analyzed through a series of mutations. The first set of mutations were designed to remove each half of the salt bridge, one at a time. The second set of mutations were designed to rescue function by utilizing a charged amino acid which differed from the wild type sequence. Finally, the last set of mutations were designed to restore the salt bridge by swapping the two residues. It was found that mutations of E185 consistently resulted in nonfunctional channels, which has been found previously in both RDL and GABA_A channels, both of which suggest a bridge from E185-R241. The electrophysiological results, accompanied by the model generated, are supported by the literature and suggest that this bridge is present in Hco-UNC-49B as well. A salt bridge may be present between R241-E183 based on literature. However, our model suggests that E183-K181 is too far away for this to occur. Further experimentation will be required to determine if there is a novel salt bridge at this location. Finally, two salt bridges were proposed to be participating with D83. This included D83-H137 and D83-R159. Based on the research on H137 in other GABA receptors it is thought to play a role in ion selection and does not participate in a salt bridge. The electrophysiological results suggest that D83 may be participating in an interaction with R159. While our model demonstrates a potential interaction the nature of this interaction requires further study. However, it is clear that both residues (D83 and R159) are critical for receptor function.

The Hco-UNC-49B/C receptor is unique and functions differently from other RDL like receptors and vertebrate GABA_A receptors. Because of this, Hco-UNC-49B/C shows promise as

a new target for anthelmintic drugs. Not only does Hco-UNC-49B/C demonstrate a unique pharmacological profile compared to other known GABA receptors (Kaji et al., 2015), it may also have unique structural differences that explain functional differences. Characterization of the channel through intramolecular and intermolecular interactions may help in uncovering the structural and functional differences of Hco-UNC-49B/C and elicit how they may be used as a drug target. While this thesis revealed the interactions between some of the conserved charged residues of Hco-UNC-49B, there are still many to be investigated. The knowledge found in this investigation of the structure of Hco-UNC-49B will widen the understanding of a unique class of GABA receptor and should validate its importance as an anthelmintic target.

References

10. References

Alexander SPH, Mathie A, Peters JA (2011). Guide to Receptors and Channels (GRAC), 5th edn. *Br J Pharmacol* 164 (Suppl. 1): S1–S324.

Accardi, M., Beech, R., Forrester, S. (2012) Nematode cys-loop GABA receptors: biological function, pharmacology and sites of action for anthelmintics. *Invert Neurosci.* 12:3-12

Accardi, M., Forrester, S. (2011) The *Haemonchus contortus* UNC-49B subunit possesses the residues required for GABA sensitivity in homomeric and heteromeric channels. *Mol Biochem Parasitol* 178 (2011) 15-22

Ashby, JA., McGonigle, IV., Price, KL., Cohen, N., Comitani, F., Dougherty, DA., Molteni, C., Lummis, SC. (2012) GABA Binding to an insect GABA receptor: A molecular dynamics and mutagenesis study. *Biophys J.* 103(10):2071-81

Bamber, B., Beg, A., Twyman, R., Jorgensen E. (1999) The *Caenorhabditis elegans* unc-49 locus encodes multiple subunits of a heteromultimeric GABA receptor. *J Neurosci.* 19(13):5348-5359.

Bamber, B., Richmond, J., Otto, J., Jorgensen, E. (2005) The composition of the GABA receptor at the *Caenorhabditis elegans* neuromuscular junction. *Br J Pharmacol.* 144 (4):502-509.

Bergmann, R., Kongsbak, K., Sorensen, P., Sander, T., Balle, T. (2013) A Unified model of the GABA_A Receptor Comprising Agonist and Benzodiazepine Binding Sites. *PLOS One*. 8 (1)e52323

Bosshard, H., Marti, D., Jelesarov, I. (2004) Protein stabilization by salt bridges: concepts, experimental approaches and clarification of some misunderstandings. *J. Mol. Recognit.* 17: 1-16

Boileau, A., Evers, A., Davis, A., Czajkowski, C. (1999) Mapping the Agonist binding site of the GABA_A Receptor: Evidence for a β -Strand. *J Neurosci.* 19(12):4847-4854

Webb, B., . Sali, A., Comparative Protein Structure Modeling Using Modeller. Current Protocols in Bioinformatics, John Wiley & Sons, Inc., 5.6.1-5.6.32, 2014.
(<https://salilab.org/modeller/>)

Connolly, C., Wafford, K. (2004) The Cys-loop superfamily of ligand-gated ion channels: the impact of receptor structure on function. *Biochem Soc Trans.* 32 (3) 529-535

Coyne, M.J. and Smith, G. (1992) The mortality and fecundity of *haemonchus contortus* in parasite-naïve and parasite-exposed sheep following single experimental infections.
Int.J.Parasitol. (22) 315-325

Crump, A., Omura, S. (2011) Ivermectin, 'Wonder drug' from Japan: the human use perspective. *Proc Jpn Acad Ser B Phys Bio Sci.* 87(2): 13-28.

Donald, J., Kulp, D., DeGrado, W. (2011) Salt Bridges: Geometrically specific, designable interactions. *Proteins.* 79 (3) 898-915

Dunne, EL., Hosie, AM., Woollorton, JR., Duquid, IC., Harvey, K., Moss, SJ., Harvey, RJ., Smart, TG. (2002) An N-terminal histidine regulates Zn(2+) inhibition on the murine GABA(A) receptor beta3 subunit. *Br J Pharmacol.* 137(1):29-38

Forrester, S., Prichard, R., Beech, R. (2002) A glutamate-gated chloride channel subunit from *haemonchus contortus*: expression in a mammalian cell line, ligand binding, and modulation of anthelmintic binding by glutamate. *Biochem Pharmacol.* 63(6)1061-8

Harder, A., Schmitt-Wrede, HP., Krucken, J., Marinovski, P., Wunderlich, F., Willsion, J., Amliwala, K., Holden-Dye, L., Walker, R., (2003) Cyclooctadepsipeptides--an anthelmintically active class of compounds exhibiting a novel mode of action. *Int J Antimicrob Agents.* 22(3):318-31

Holden-Dye, L., Walker, R. (2014) Anthelmintic drugs and nematicides: Studies in *Caenorhabditis elegans*. *WormBook: ed*. Doi:10.1895/wormbook.1.143.1 retrieved from: <http://www.ncbi.nlm.nih.gov/books/NBK116072/>

Kaji, M., Kwaka, A., Callanan, M., Nusrat, H., Desaulniers, JP., Forrester, S. (2015) A molecular characterization of the agonist binding site of a nematode cys-loop GABA receptor. *Br J Pharmacol*. 172, 3737-3747

Kaminsky,R., Ducray,P., Jung,M., Clover,R., Rufener,L., Bouvier,J., Weber,S.S.,

Wenger,A., Wieland-Berghausen,S. and Goebel,T. (2008). A new class of anthelmintics effective against drug-resistant nematodes. *Nature* (452) 176-180

Lacey, E. (1990) Mode of Action of benzimidazoles. *Parasitol Today*. 6 (4):112-5

Manninen and Oksanen: Haemonchosis in a sheep flock in North Finland. *Acta Veterinaria Scandinavica* 2010 52(Suppl 1)519.

Miller, P., Aricescu, A. (2014) Crystal Structure of a Human GABA A Receptor. *Nature*. 512: 270-275.

Newell, JG., McDevitt, RA., Czajkowski C. (2004) Mutation of Glutamate 155 of the GABAA Receptor B 2 subunit produces a spontaneously open channel: A trigger for channel Activity. *J Neurosci.* 24(50):11226-35

Nikolaou, S. and Gasser, R.B (2006) Prospects for exploring molecular developmental process in *Haemonchus contortus*. *Int.J.Parasitol.* (36) 859-868

Nys, M., Kester, D., Ulens, C. (2013) Structural insights into cys-loop receptor function and ligand recognition. *Biochem. Pharmacol.* 86 (2013) 1042-1053

O'Connor, L., Walkden-Brown, S., Kahn, L. (2006) Ecology of the free-living stages of major trichostrongylid parasites of sheep. *Vet Parasitol.* 142 (2006) 115

Pestechian, N., Kalani, H., Faridnia R., Yousefi H., (2014) Zoonotic gastrointestinal Nematodes (Trichostrongylidae) from Sheep and Goat in Isfahan, Iran. *Acta Scientiae Veterinariae.* 42: 1243

Pettersen EF, Goddard TD, Huang CC, Couch GS, Greenblatt DM, Meng EC, Ferrin TE. J (2004) UCSF Chimera--a visualization system for exploratory research and analysis. *Comput Chem.* 2004 Oct;25(13):1605-12.

Qamar, M., Maqbool, A., Ahmad, N. (2011) Economic Losses due to Haemonchosis in sheep and goats. *Sci. Int.* 23(4),321-324

Roberts, L., J. Janovy. 2000. Foundations of Parasitology. US: The McGraw Hill Companies, Inc..

Roeber, F., Jex, A., Gasser, R., (2013) Impact of gastrointestinal parasitic nematodes of sheep, and the role of advanced molecular tools for exploring epidemiology and drug resistance- an Australian perspective. *Parasit Vectors.* 6:153

Saras, A., Gisselmann, G., Voqt-Eisele, AK., Erlkamp, KS., Kletke, O., Pusch, H., Hatt, H. (2008) Histamine action on vertebrate GABA receptors: direct channel gating and potentiation of GABA responses. *J Biol Chem.* 18; 283(16) 10407-5.

Schuske, K., Beg, A., Jorgensen, E. (2004) The GABA nervous system in *C. Elegans*. *Trends Neurosci.* 27 (7) 407-415

Siddiqui, S., Brown, D., Vijayaraghava, T., Forrester, S. (2010) An UNC-49 GABA receptor subunit from the parasitic nematode *Haemonchus contortus* is associated with enhanced GABA sensitivity in nematode heteromeric channels. *J Neurochem.* 113: 1113-1122

Sigel, E., Steinmann, M. (2012) Structure, Function and Modulation of GABA_A Receptors. *J Biol Chem.* 287(48):40224-31

Schwarz, E., Korhonen, P., Campbell, B., Young, N., Jex, A., Jabbar, A., Hall, R., Mondal, A., Howe, A., Pell, J., Hofmann, A., Boag, P., Zhu, X., Gregory, T., Loukas, A., Williams, B., Antoshechkin, I., Brown, C., Sternberg, P., Gasser, R. (2013) The genome and developmental transcriptome of the strongylid nematode *Haemonchus contortus*. *Genome Biol:* 14:R89

Thompson, AJ., Lester, HA., Lummis, SC. (2010) The structural basis of function in Cys-loop receptors. *Q Rev Biophys:* 43 (4)449-99

Unwin, N (1993) Neurotransmitter action: opening of ligand-gated ion channels. *Cell.* 72 Suppl:31-41

Veglia, F.(1915) The Anatomy and Life-history of the *Haemonchus Contortas* (Rud). *Veterinary Research Laboratories, Onderstepoort.*

Venkatachalan, S., Czajkowski, C., (2009) A conserved salt bridge critical for GABA_A receptor function and Loop C dynamics. *PNAS.* 106 (15) 13604-13609

Appendices

11. Appendices

The following appendix highlights the primers used in this study and additional experimentation and results achieved during my studies at UOIT.

11.1. Primers for the mutants generated for intramolecular analysis

Table 1. Hco-UNC49B charged residue mutagenesis Primers. Each mutagenesis primer name indicates the residue to be mutated, the position in the sequence, and the new residue in the mutant. Primers were designed using Stratagene's web-based QuikChange® Primer Design Program.

Mutagenesis	Forward Primer (sense)	Reverse primer (antisense)
Primer Name		
Single Substitution Mutations		
D83A	5'-TGGATATGGACTTT ACGCTAGCTTTCTAT -3'	5'CATGTTTGTTCGCATATAGAAAGC TAGCGT-3'
D83E	5'-CCATGTTTGTTCGCAT ATAGAACTCTAGCGT AAAGTCCATATCC-3'	5'-GGATATGGACTTTAC GCTAGAGTTCTATATGCGACAAAC ATG -3'
D83T	5'- GCCATGTTTGTTCGCATAT AGAAAGTTAGCGTAAAG TCCATATCCACTT -3'	5'- AAGTGGATATGGACTTTACGCTAA CTTTCTATATGCGACAAACATGGC - 3'
E183A	5'-GTATAGCAATAGCTT TCAATTGCCAGCTT -3'	5'-ATTCACAACGATGCA AGCTGGCAATTG A-3'
E185A	5'- CCATTGTATAGCAATAG	5'- ACGATGCAAGCTGGAAATTGCAAG CTATTGCTATACAATGG-3'

	CTTGCAATTTCCAGCTTG CATCGT-3'	
E185D	5'- GTATAGCAATAGCTATC AATTTCCAGCTTGCATC GTTGTGA -3'	5'- TCACAACGATGCAAGCTGGAAATT GATAGCTATTGCTATAC-3'
H137A	5'- TGCGTTGTGGCCAAGGC GAAAAACGATT-3'	5'- CGAACGAGAAGAAATCGTTTTTCG CCTTG-3'
H137K	5'- ATGCGTTGTGGCCAACT TGAAAAACGATTTCTTC TCGTTCG-3'	5'- CGAACGAGAAGAAATCGTTTTTCA AGTTGGCCACAACGCAT-3'
R159A	5'- CGGTGACCGTAAGCGCT TGACTAGTGTA-3'	5'- ACGGTCTACACTAGTCAAGCGCTT ACGG-3'
R159K	5'- GCGGTGACCGTAAGCTT TTGACTAGTGTAGACCG TG-3'	5'- CACGGTCTACACTAGTCAAAAGCT TACGGTCACCGC-3'
R241A	5'- GAGAAGAATTTCAAAGT ATAAAGCCCTAT-3'	5'- CACATCATCAGGGTCGTATAGGGC TTAT-3'
R241K	5'- CTGACGAGAAGAATTTT AAAGTATAACTTCTAT ACGACCCTGATGATGTG GTTG-3'	5'- CAACCACATCATCAGGGTCGTATA GGAAGTTATACTTTGAAATTCTTCT CGTCAG-3'

Swap Mutation Primers

D83H	5'- ATGTTTGTTCGCATATAG AAATGTAGCGTAAAGTC CATATCCAC-3'	5'- GTGGATATGGACTTTACGCTACATT TCTATATGCGACAAACAT-3'
-------------	--	---

H137D	5'- CGTTGTGGCCAAGTCGA AAAACGATTTCTTCTCGT T-3'	5'- AACGAGAAGAAATCGTTTTTCGAC TTGGCCACAACG-3'
D83R	5'- CCATGTTTGTGCGCATATA GAAACGTAGCGTAAAGT CCATATCCACT-3'	5'- AGTGGATATGGACTTTACGCTACG TTTCTATATGCGACAAACATGG-3'
R159D	5'- ATGTGGCGGTGACCGTA AGATCTTGACTAGTGTA GACCGTG-3'	5'- CACGGTCTACACTAGTCAAGATCT TACGGTCACCGCCACAT-3'
E185R	5'- CCATTGTATAGCAATAG CTTCTAATTTCCAGCTTG CATCGTTGTGAATC-3'	5'- GATTCACAACGATGCAAGCTGGAA ATTAGAAGCTATTGCTATAACAATG G-3'
R241E	5'- GACGAGAAGAATTTCAA AGTATAACTCCCTATAC GACCCTGATGATGTGGT- 3'	5'- ACCACATCATCAGGGTCGTATAGG GAGTTATACTTTGAAATTCCTTCG TC-3'

11.2. Characterization of Loop E residues utilizing the Substituted Cysteine Accessibility Method

Previously, Substituted Cysteine Accessibility method (SCAM) was performed on the first half of Loop E and demonstrated a number of important residues. In order to fully understand this loop's participation with GABA, the residues D151, G152, T153, V154, and R159 were analyzed. Of the five mutants tested and modified by MTSET, only two, T153C and R159C effected GABA activation (caused an increased response). It is interesting to note that both of these residues are predicted to line the binding site of GABA_A utilizing SCAM (Bergmann et al., 2013). T153C showed a $143\% \pm 9.85$ response after MTSET relative to its response to GABA, and R159C showed a $128\% \pm 5.82$ response relative to GABA.

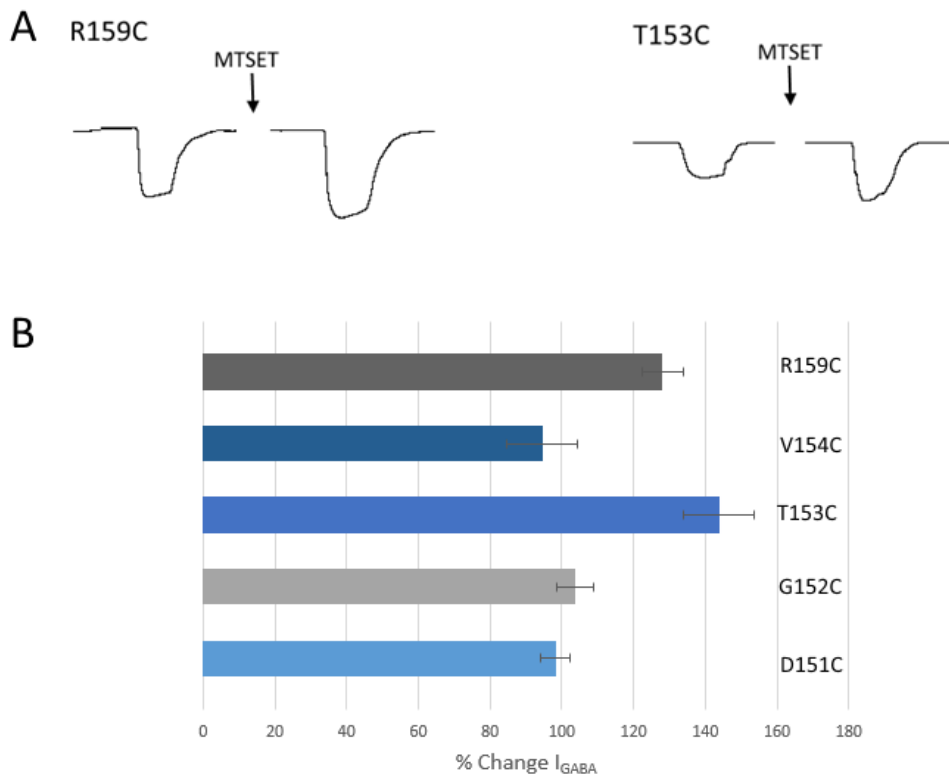


Figure 1. A: Representative responses before and after MTSET for R159C and T153C at their respective EC_{50} values. B: comparison of the percent change of I_{GABA} for each SCAM mutation

11.3. Characterization of Hco-UNC-49 utilizing GABA Analogues

In order to further characterize the wild-type Hco-UNC-49 B/C receptor, a number of compounds were developed (Forrester and Desaulniers, unpublished data). These compounds were composed of six GABA analogues (Appendices Table 2), and analyzed through electrophysiological studies as previously described. Of the six analogues created, only two demonstrated the ability to activate the receptor. These two molecules, (E)-3-carboxyprop-2-en-1-aminium (TACA), and 4-(hydroxyamino)-4-oxobutan-1-aminium showed comparable

responses to activation by GABA. In order to further analyze these analogues, EC₅₀ were calculated using electrophysiology.

Table 2. GABA analogues to be used on the WT (wild-type) UNC-49 channel of *H. contortus*.

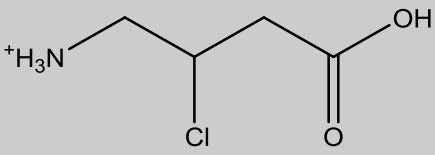
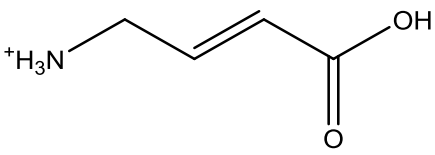
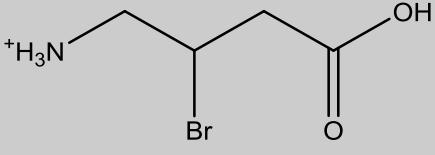
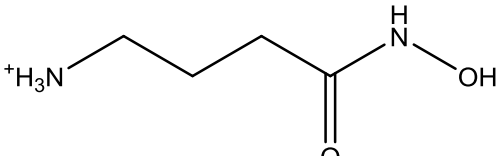
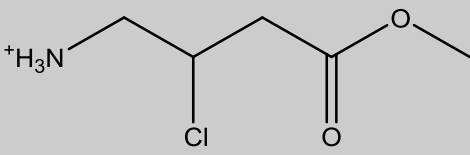
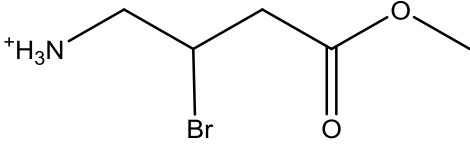
Compound Name	Structure
3-carboxy-2-chloropropan-1-aminium	
<i>(E)</i> -3-carboxyprop-2-en-1-aminium	
2-bromo-3-carboxypropan-1-aminium	
4-(hydroxyamino)-4-oxobutan-1-aminium	
2-chloro-4-methoxy-4-oxobutan-1-aminium	
2-bromo-4-methoxy-4-oxobutan-1-aminium	

Table 3. EC₅₀ calculations of the two GABA analogues known as Molecule B (TACA) and Molecule D (4-(hydroxyamino)-4-oxobutan-1-aminium) are compared to the heteromeric UNC-49B/C receptor with GABA.

Compound	EC ₅₀ ± S.E. (μM)	Number of oocytes
Wild-Type	68.03±17.3	6
Molecule B (TACA)	290.4 ± 15.05	9
Molecule D	194.3 ± 8.239	8

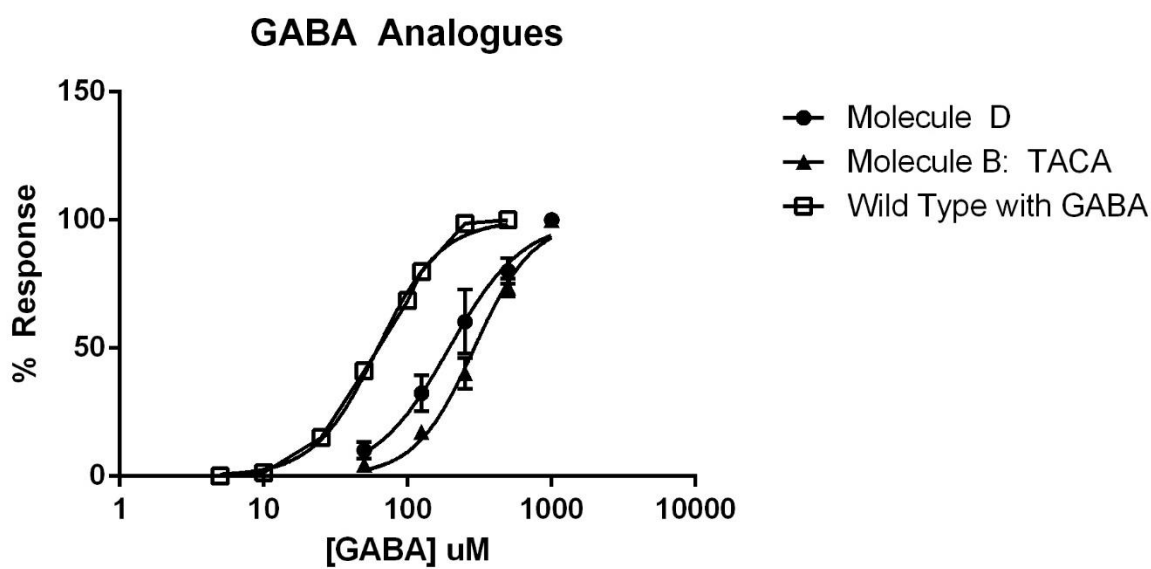


Figure 2. Dose response curves for the two GABA analogues, Molecule B (TACA) and Molecule D (4-(hydroxyamino)-4-oxobutan-1-aminium).

11.4. *Pharmacological study of D83T*

Due to the fact that D83 showed such interesting results with the knock out D83A mutation and because a functional GABA_A β3 homomeric receptor maintains activity while lacking D83, it was decided to that the potential function of this residue would be investigated. In order to achieve this, three other agonists were analyzed: IMA, R-GABOB and S-GABOB, as well as one

inhibitor, gabazine. These agonists were used to determine if they could elicit a full agonistic response in the D83T receptor by comparing each compound at 10mM, as indicated in Appendices Figure 3. IMA acted as a full agonist with responses on average being higher than that of GABA, at 110% relative to maximal GABA concentrations. R-GABOB nearly functioned as a full agonist with an average 78.5% response. Finally S-GABOB demonstrated only partial agonistic effect showing only 54% that of a maximal GABA response. The antagonist gabazine also caused a 49% reduction in the GABA response at the D83T receptor.

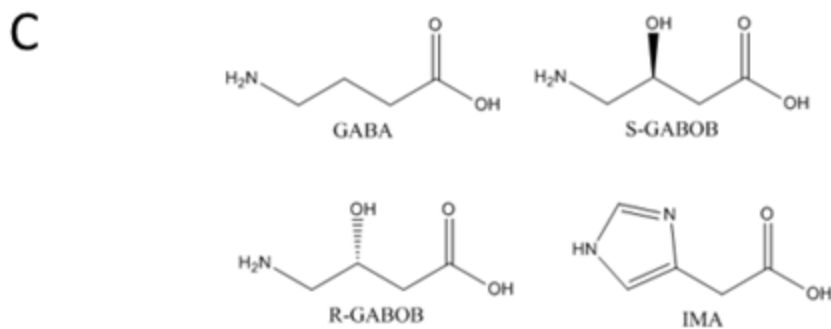
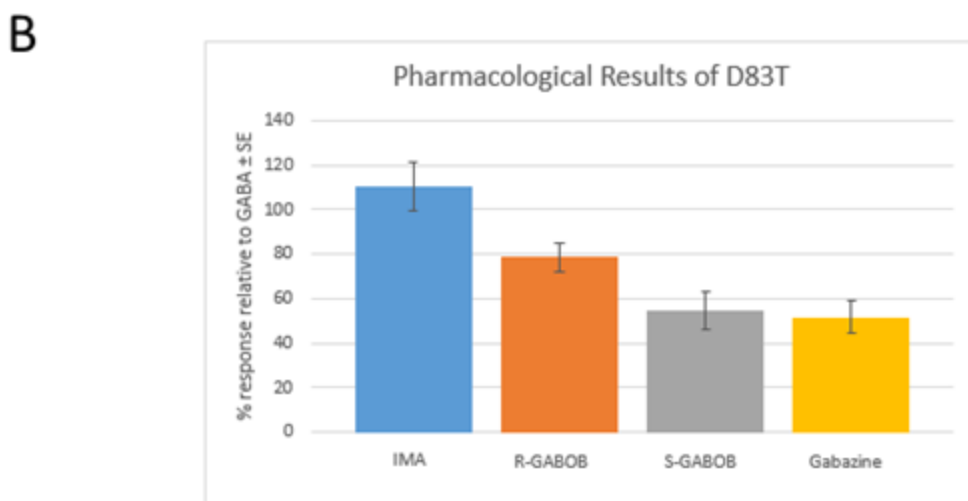


Figure 3. A: Representative responses of D83T with GABA, IMA, R-GABOB and S-GABOB at 10mM. EC₅₀ responses for D83T shown with Gabazine underneath. B: Pharmacological results of D83T comparing the responses of each compound relative to GABA. C: Chemical structures of GABA, S-GABOB, R-GABOB and IMA